ETH
Eidgenössische Technische Hochschule Zürich
Swiss Federal Institute of Technology Zurich

eeh power systems laboratory

Viktor Lenz

Generation of Realistic Distribution Grid Topologies Based on Spatial Load Maps

Semester Thesis
PSL 1434

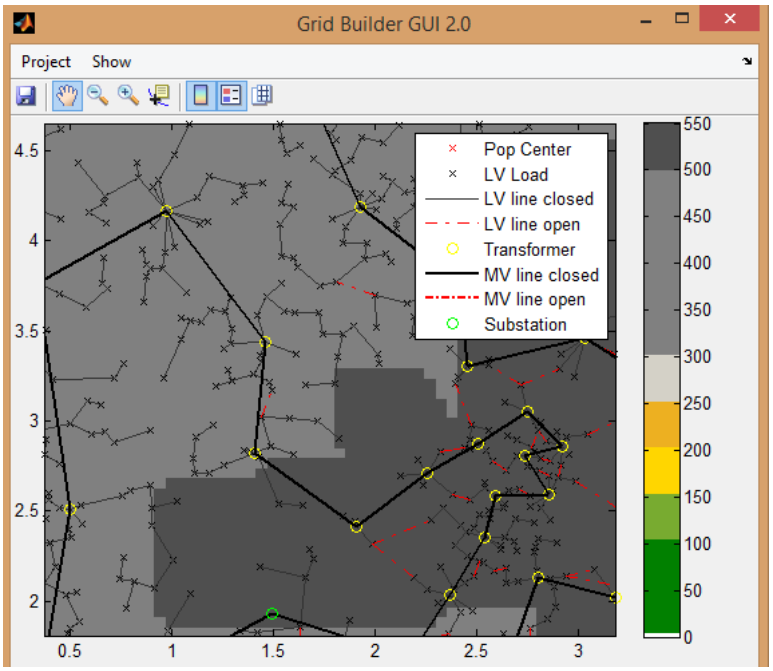

EEH – Power Systems Laboratory
Swiss Federal Institute of Technology (ETH) Zurich

Examiner: Prof. Dr. Göran Andersson
Supervisor: Dr. Stephan Koch, Dr. Osvaldo Rodríguez Villalón

Zurich, April 28, 2015

ADAPTRICITY

Abstract

In the framework of a distribution system simulation software a MATLAB module that generates synthetic benchmark distribution grid topologies is developed.
By analysing the grid data of distribution system operators the distribution grid type (topological configuration, transformer size, loads) is linked to the spatial population density allowing an simple but efficient generation of different distribution grids. For increased user-friendliness a GUI provides the possibility to draw a spatial population density distribution based on which a distribution grid is generated.
The module then calculates the number of necessary transformer stations and connects LV loads in radial or partly open-ring configuration using a modified minimum spanning tree algorithm before dimensioning lines and transformers in order to allow secure operation. On the MV level a vehicle routing problem algorithm connects the transformer stations in rings to the distribution grid's substation.

Contents

List of Acronyms **iv**

1 Introduction **1**
1.1 Motivation . . . 1
1.2 Goals . . . 2
1.3 Overview of the field . . . 2
1.4 Thesis overview . . . 2

2 Theory **3**
2.1 Distribution grid characteristics . . . 3
2.1.1 International Comparison . . . 4
2.1.2 Medium voltage distribution networks . . . 5
2.1.3 Low voltage distribution networks . . . 6
2.1.4 Reliability levels . . . 6
2.1.5 Differentiation by geographic area . . . 7
2.2 Distribution grid components . . . 8
2.2.1 Loads . . . 9
2.2.2 Transformers . . . 11
2.2.3 Lines . . . 15
2.3 Power line routing . . . 17
2.3.1 LV system . . . 17
2.3.2 MV system . . . 19

3 Implementation **20**
3.1 Data . . . 20
3.1.1 Input . . . 20
3.1.2 Output . . . 20
3.2 Graphical user interface . . . 23
3.2.1 Chart . . . 25
3.2.2 Table . . . 25
3.2.3 Toolbar . . . 25
3.2.4 Menu bar . . . 25
3.3 Generation of a distribution grid . . . 26

3.3.1 Modeling of a spatial load map 26
3.3.2 Generation of the LV distribution grid 28
3.3.3 Generation of the MV distribution grid 31

4 Results and discussion **35**
4.1 Testing device 35
4.2 Spatial load map 35
4.2.1 Results 36
4.2.2 Load computation time 37
4.2.3 Scope for improvement 37
4.2.4 Commercial/industrial/MV loads 42
4.3 LV distribution grid 42
4.3.1 Results 42
4.3.2 LV grid computation time 47
4.3.3 Scope for improvement 47
4.4 MV distribution grid 49
4.4.1 Results 49
4.4.2 MV grid computation time 50
4.4.3 Scope for improvement 50

5 Conclusion and future work **52**

A Settlement classification **53**
A.1 BSSR classification (Germany) 53
A.2 Grid characteristics [1] and [2] 54
A.2.1 Transformer characteristics 54
A.2.2 Load characteristics 54
A.2.3 Line characteristics 55
A.3 Grid structure German DSO database 55

B Load modeling **57**

C Line dimensioning **58**

D Software module **59**
D.1 Parameters 59
D.2 GUI handling of data 60
D.3 Grid building procedure 61

Bibliography **65**

List of Acronyms

DS distribution system

DSO distribution system operator

TS transmission system

TSO Transmission system operator

LV low voltage

MV medium voltage

HV high voltage

TSt transformer station

SSt substation

CP connection point

ACl areal class

MST minimum spanning tree

TSP travelling salesman problem

VRP vehicle routing problem

RES renewable energy sources

OHL overhead line

SLP standard load profile

Chapter 1

Introduction

This semester project covers the development of software that generates realistic distribution grid topologies. The ETH spin-off *Adaptricity* assigned this task in the framework of their distribution system simulation software *DPG.sim*. To comprehensively illustrate the ambition and importance of this project the following four sections (1) explain the motivation for this project, (2) define the objectives (3) discuss related projects from other institutions and (4) give an overview of the thesis' structure.

1.1 Motivation

Up to now distribution systems (DSs) are designed such that neither the maximum power generation nor the maximum power consumption violates the grid loading limits. Because of an increasing share of renewable energy sources (RES) connected directly to the DG, it is questionable if the currently applied worst-case grid design is appropriate.
In search for an optimal grid design *Adaptricity* is developing the distribution system simulation software *DPG.sim*. This software allows realistic active DS and smart grids operation simulation as well as analysis of the temporal evolution of generation, load, storage states, and of operational control algorithms. *DPG.sim* helps distribution system operators (DSOs) to evaluate the integration of *smart-grid elements* in their system with a high precision and gives academia the possibility to assess novel methods for *smart-grids* and *active distribution network management* [3].
As DSOs hardly ever publish their exact grid structure most academic optimization methods have to be verified with generic benchmark grids (low voltage (LV) [4, 5]; medium voltage (MV) [6]). To offer academic research a larger range of realistic distribution grid a software module that generates reference grids of arbitrary size is highly desirable.

1.2 Goals

In order to develop a software module for the generation of realistic distribution grid topologies the following goals have to fulfilled:

- A characterization of different types of distribution grids
- Modeling spatial maps with a certain spatial load distribution
- Generation of a distribution grid for a given spatial load distribution in an "open-ring" configuration
- Dimensioning the lines by nominal load
- Documentation of the project

Although the programming and modeling is done in MATLAB it is important to keep a structure which is easily transferable to JAVA, so that it can later be implemented into *DPG.sim*.

1.3 Overview of the field

Up to now no finished software or complete algorithm that provides a realistic MV/LV DG structure seems to exist.
A group at TU Kaiserslautern is working on *Synthetic Medium Voltage Grids* by constructing 10 different exclusive cases of regional load distribution in a spatial load map [7]. Unfortunately several important steps, as the line routing algorithm, dimensioning of transformers and the sizing of the cables, are not or only vaguely described. But this work inspired the idea of the user drawing a spatial population density map.
Another collaboration developed *A random growth model for power grids* to create synthetic transmission networks including a dynamic growing phase. Their approach of using the minimum spanning tree (MST) algorithm inspired the application of the MST in this work [8].

1.4 Thesis overview

This report has the intention of both introducing the concept of generating distribution grids in theory and explaining the handling of the software module to readers and users. In Chapter 2 the general characteristics of distribution grids, their components and common dimensioning approaches are explained. Chapter 3 guides trough the module's application and explains the algorithms in use. The software's functionality was tested and verified for different population densities as described in Chapter 4. Chapter 5 concludes the report with a resume of the work done and sets the scope for future work.

Chapter 2

Theory

In this chapter the characteristics and differences of typical DSs and the modeling of the grid's components are explained to provide the origin of both the used parameters and the formulas used in the implementation.
Main sources for the presented theory are academic publications and technical reports from industry in the field.
In addition a database of all German DSOs' system data was available, which the operators are obliged to publish according to German law ([9, 10]). Unfortunately around 100 of the 853 recorded DSO data sets were corrupted by missing, incorrect or obsolete numbers. Data sets from 32 DSOs were updated in line with this project from either their website or by directly contacting them by phone or mail. Another 10 DSOs did not respond to these requests. Consequently as it was not possible to collect useful data for all DSOs or to sort out all corrupted data the evaluated key characteristics given by their average values in Appendix A.3 have to be used with caution.

2.1 Distribution grid characteristics

A distribution grid comprises all the power lines and cables, transformers, protection, switchgear, control and metering devices that extract electrical energy from the high voltage (220 kV to 380 kV) transmission systems (TSs) and then transport and distribute it to the end consumers. Coming from the transmission grid, the demanded energy's voltage level is stepped down from high voltage (HV) to MV at substations (SSts). In the MV grid the energy then is transmitted to local distribution transformer stations (TSts) via distribution cables or overhead lines (OHLs). At the TSts the voltage is transformed to the consumer level (LV) and distributed via feeders. At the feeders' connection points (CPs) service laterals branch off and carry the electricity to homes, public places and commercial buildings. The DSOs are responsible for managing and servicing distribution grids.
To provide a basic understanding of the distribution grid structures (1) the

Table 2.1: Distribution voltages for North America and Europe [11]

Type of voltage	North America	Europe
MV three-phase	4 kV to 35 kV	6.6 kV to 33 kV
LV three-phase	208, 480, or 600 V	380, 400 or 416 V
LV single-phase	**120**/240, 277 or 347 V	220, **230** or 240 V

properties of typical European DSs are described and compared to the DSs in the US, (2) the MV and the (3) LV-grid topology are explained before (4) the region type specific differences of DS-layouts in Germany are outlined.

2.1.1 International Comparison

The European system and the North American system are the two most popular power distribution systems in the world. The main difference are the higher voltages on the distribution level (Table 2.1) used in the European system which lead to different construction principles:

- To reduce losses the American system maximizes the MV network by reducing the length of LV cables. In addition the MV grid has a neutral with regular earthing and the main branch is three-phase and of radial structure with one- to three-phase branches where the MV/LV TSts are connected to.
- The European system on the other hand allows longer LV conductors, the MV is three-phase without distributed neutral, the neutral earthing is either solid or via impedance at the HV/MV substations and the network is of either radial or ring structure.

Compared to the North American system the European system shows both advantages and disadvantages [11]:

Advantages Higher power carrying capacity at given ampacity, less voltage drop, less line losses. As a consequence the supplied area can be wider and less (but higher rated) SSts are needed.

Disadvantages Longer circuits reduce the reliability level and increase the risk of a customer interruption in case of a fault. Concerning the costs the system equipment (larger dimensioned TSts and reliability means) is more expensive.

This project sets focus on the German (European) distribution grids for two reasons: (1) *DPG.sim* is mainly intended for European DSs and (2) German DSOs provide the largest dataset and geographic variety to identify and verify relevant parameters.

2.1.2 Medium voltage distribution networks

German medium voltage grids (*primary* distribution) operate at 10 kV in urban areas or at 20 kV in rural areas.
They obtain the energy via substations with HV/MV-transformers from 110 kV high voltage networks. The medium voltage grid distributes the in-fed power from the SSt to the TSts (MV/LV-transformer) and to the industrial bulk consumers.
For connecting the TSts with the power supplying SSts, three different structures are used in Germany. The choice depends on the projected reliability level, the location of the transformers and the line routing possibilities.

Radial configuration

The simplest structure is the radial configuration which is characterized by having only one path for power to flow from the source (SSt) to each customer (TSt). The main feeders are connected via circuit breakers to the bus-bar on the 10 kV-MV-winding of a 110 kV to 10 kV substation. Each of these feeders exclusively feeds several TSts (connected via load break switches). Figure 2.1 a) shows a radial structure.

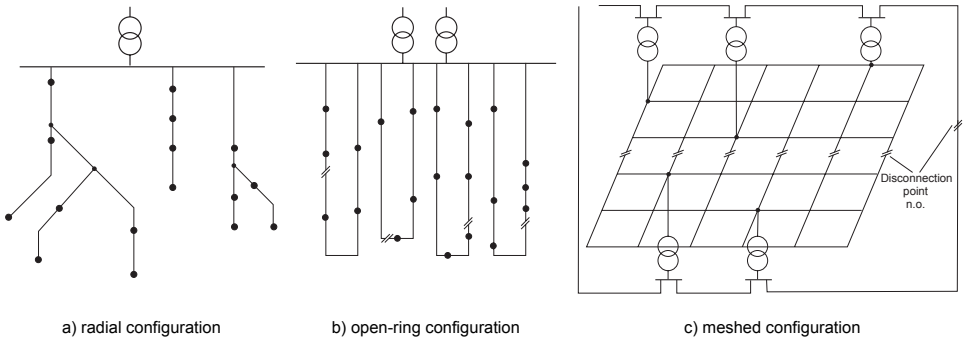

Figure 2.1: Examples of a) radial, b) ring and c) meshed configuration [12]

Open-ring configuration (one substation)

Distribution networks in open-ring configuration increase the reliability of supply by the option to connect two main feeders from one substation (now called half-rings) with each other, see Figure 2.1 b). During normal operation the switch connecting the half-rings is open, in case of a disturbance the affected device or conductor section is disconnected and the connection switch is closed to ensure supply of all operable TSts. This configuration is useful for areas with high load density and a centrally placed SSt.

Open-ring configuration (two substations)

In the cases of elongated areas, long straight cable routes or outlying SSts it is recommended to construct an open ring structure between two different SSts. In this configuration the two half-rings start at two different neighboring SSt (which are connected via the HV grid). The switching procedure is similar to switching with only one SSt.

2.1.3 Low voltage distribution networks

German local low voltage grids (secondary distribution) operate at 400 V and spread out from a single TSt (MV/LV).
A TSt's supply radius is between 250 m to 500 m depending on its rated apparent power S_r (100 kVA to 630 kVA). This corresponds to 30 to 500 residential units, the radius of the supply area is limited by voltage drop limits along the lines.
In addition to the transformer, cable distribution cabinets with 4 to 8 outlets are placed at crossroads. This allows an individual disconnection of malfunctioning sub-feeders while the main feeder maintains normal operation.
Although the reliability level decreases from meshed[1] over open-ring to radial configuration [11] the radial configuration is because of its easy and clear operation the most practical configuration [13, 1].

2.1.4 Reliability levels

According to [11] European distribution systems can classified by one out of three reliability levels:

Reliability level 1

- MV: each transformer is connected to the source through two feeders (one is a standby to the other)
- LV: one of the following configurations
  - open-ring
  - combination open-ring with double radial
  - double radial supplied by a double TSt
  - double radial supplied by two TSts
  - closed-ring
  - semiclosed-ring
- fast automation technique

[1] The meshed configuration completes the open-ring concept of double supply so that all nodes and branches are connectable to multiple supplies, see Figure 2.1 c).

- backup generators to supply very critical loads

Reliability level 2

- MV: as for level 1
- LV: one of the following configurations
  - open-ring
  - combination open-ring with double radial
  - double radial supplied by a double TSt
  - double radial supplied by two TSts

Reliability level 3

- MV: as for level 1
- LV: Radial feeders. If a fault occurs on these feeders all load behind the fault is disconnected.

As it was explained in the above sections, LV grids are preferably run in radial and MV grids in open-ring configuration.
Comparing the three different reliability levels it is obvious that in all three cases, the MV connection must be at least in open-ring structure.
The LV level can be realized in radial configuration for all three reliability levels with the difference that for reliability level 1 and 2 the TSt has to be equipped with a standby transformer and a second standby line in parallel to the radially laid lines of reliability level 3.
A distribution network consisting of radial LV structures and an open-ring MV structure can meet the requirements of each of the three reliability levels without modifying the topology (but doubling the transformer power and total line length).
This network concept is chosen for this project in order to both avoid a complicated structure and offer all three reliability levels at the same time.

2.1.5 Differentiation by geographic area

The load density of a supplied area has critical impact on the characteristics of the grid so that grid types can be differentiated by the regional load density [13].
Scheffler showed that specific load densities can directly be linked to certain settlement patterns. In addition he identified characteristic variables for low voltage distribution grids for each of the defined settlement patterns [1].
Some of these variables will be used for our generic distribution grids either for the construction, as *the rated TSt power, the number of feeders leaving*

the station (Appendix A.2), or the verification of the model, e.g. *length of the feeders, conductor material of the feeders, distance between connected buildings.*
However Scheffler's settlement patterns only hold for areas between 6 ha to 60 ha and their classification is done by only soft criteria.
The *Bundesinstitut für Bau-, Stadt- und Raumplanung (BSSR)* on the other hand offers a classification of counties and regions by population density [14] allowing a better mapping of the regional observations made by [13] and [15].
Using the *number of housing units per connected building* and the average *area per building* from Scheffler it was possible to merge each population density class with its most common settlement pattern by Scheffler to seven *areal classes (ACls).*
The resulting ACl classification which is used in this project for modeling different settlements is listed in Table 2.2 together with the BSSR classification and the assigned settlement patterns by Scheffler.
Figure A.1 shows the map of the BSSR classification applied on Germany.

Table 2.2: Population density classification of different regions and the most common settlement patterns

	areal	BSSR classification (modified)	
settlement pattern by [1]	**class**	area type (density)	$\frac{\text{inhabitants}}{km^2}$
scattered settlements	**R1**	rural area (low)	0-100
villages (mainly farms)	**R2**	rural area (high)	100-150
1- and 2-family houses area	**U1**	urbanized area (low)	150-200
1-family houses, village center	**U1**		
terraced housing	**U1**		
row development	**U2**	urbanized area(high)	200-250
block development	**A1**	area with agglomeration centers	250-300
medieval old town	**A2**	agglomeration	300-500
high-rise row development	**A3**	agglomeration (high)	>500

Unfortunately it was not possible to properly analyze the statistical significance of this classification using the DSO database due to the insufficient quality of the database. Determining the ACls' statistical significance is highly recommended as soon as a complete database is available.

2.2 Distribution grid components

In this section the models of the three most fundamental components of a distribution grid (1) *Loads,* (2) *Lines* and (3) *Transformers* are explained.
For a complete description of a distribution grid further elements such as

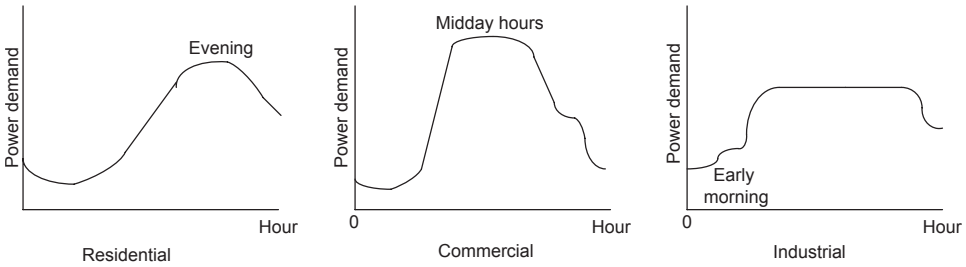

Figure 2.2: Most common DG load classes according to [11]

switches, *shunt capacitors* and *voltage regulators* as well as the *phasing* of loads and transformers have to be included [16], but these elements are not considered in this projects' basic approach of generating the fundamental structures of distribution grids.

2.2.1 Loads

A common modeling approach in literature is classifying loads (= electricity consumers) by their typical power consumption over the day respectively over the year (t-P-curves). According to Sallam et al. the most used classes are *residential, commercial* (usually LV) and *industrial* (usually directly connected to MV) [11].
Their fundamental differences are illustrated in Figure 2.2: For the residential class, the peak is almost in the evening while for the commercial class it is at midday hours. The industrial class is approximately constant from the late morning until shutting down in the afternoon.

German DSOs use so-called standard load profiles (SLPs), normalized to 1000 kWh/a, to forecast the LV consumers' demands. These SLPs, provided by the German association of energy and water industries *BDEW*, cover the 15 min consumption of one residential, seven different commercial and three types of agricultural customers. Figure 2.3 displays the most-used SLPs of each group. The residential and commerce group are similar to those by Sallam et al. , the agricultural customers have high demand during the early morning and late evening. The *BDEW* does not provide a SLP for industry but a continuous band profile.

For the planning and dimensioning of grids the most important information is the maximum power which lines have to transport and transformers have to transform at a certain time. Consequently the very necessary information about loads is their peak power demand p_{pk}, the power factor λ, which is the ratio between apparent power and active power, their yearly energy consumption E to deduce the average power demand and information about the coincidence of the loads peaks (how much each single load contributes to the coincident peak demand at a specific instant of time). The following two sections provide concrete numbers for the loads connected to the LV

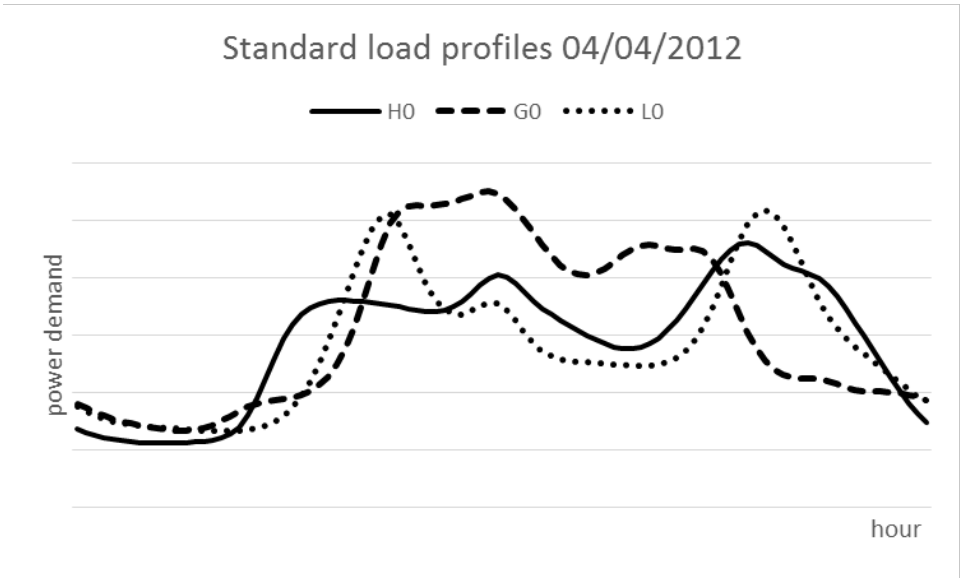

Figure 2.3: standard load profiles by the BDEW for households (H0), commerce (G0) and farms (L0)

and MV grid.

LV loads

For each of the seven different ACls a most common building type was identified in Table 2.2. It can be assumed that each of these buildings represents one connection point and has one service lateral (connection to the feeder). This means that the grid "sees" every building as one single load with one single maximum demand and one specific yearly power consumption although the building may envelope multiple households as can be seen in Table A.4. To model loads with both a certain variation and consistency this project assumes that in each ACl only the most common building type is present but the number of households in every buildings h_{cp} varies within a uniform distribution.
The typical households' yearly energy consumptions[2] E_h are listed by mean and standard deviation in Table A.3. As we already have a variation of the households the standard deviation of the yearly consumption is neglected in this project and the mean values are rounded to 100 kWh so that total yearly energy consumption E_{cp} for each class can be determined:

$$E_{cp} = h_{cp} \cdot E_h \tag{2.1}$$

The range of h_{cp} and the values for E_h are listed in Table 2.3.
In literature a wide variation of the households peak demand can be found

[2] Average size of a household in Germany 2011: 2.02. Source: *Statistisches Bundesamt*

ranging from 1.92 kW to 30 kW. A comparison is shown in Table B.2.
In this project a peak demand of 18 kW was chosen as a compromise between the more popular publications [2] and [4] and because it is based on a very practical approach [17].
Table 2.3 lists the ranges of the coincident peak demand per building $p_{pk,18kW}$ depending of the number of households in the building according to the coincidence calculation from [17].
Furthermore an attempt was made to acquire the necessary data for models of commercial (supermarkets, offices) and public (schools, town hall) LV loads. Due to the lack of statistical data (see also Chapter 5) this was not successful and non-private consumers had to be omitted for this project.

Table 2.3: Load per household and ratio of households per building by ACl

	R1	R2	U1	U2	A1	A2	A3
E_h [MWh]	3.0	3.4	4.0	1.9	2.7	2.7	1.7
h_{cp}[a] [un. dist.]	1–2	1–3	1–2	4–14	5–15	1–11	10–80
$p_{pk,18kW}$ [kW]	18–25	18–30	18–25	35–64	39–66	18–57	54–147

[a]The data from Scheffer (Table A.4) was fit into a uniform distribution with integer endpoints with a maximum variation around the given mean $|\Delta\mu| \leq 0.1\mu$.

MV loads

Literature does not provide useful information about size, amount and distribution of public, industrial and commercial buildings in MV grids. As neither general nor for the ACls-specific data was found this project can only consider private loads connected to the LV grid and assumes the MV grid to be free of loads.

2.2.2 Transformers

LV: Transformer stations

Three variables define a transformer in a distribution system map [5]: (1) the location of the transformer, (2) its rated power S_r in kVA and (3) how it is connected to the grid.

Location As explained earlier, the location on the transformer station (TSt) depends on the structure of the supplied area:
In grids of compact structure the TSt is placed as central as possible to minimize line length and thereby minimize the line losses and voltage drops. In large meshed systems with multiple redundant transformers, they are placed at the nodes with the highest load density. Depending on the reliability level

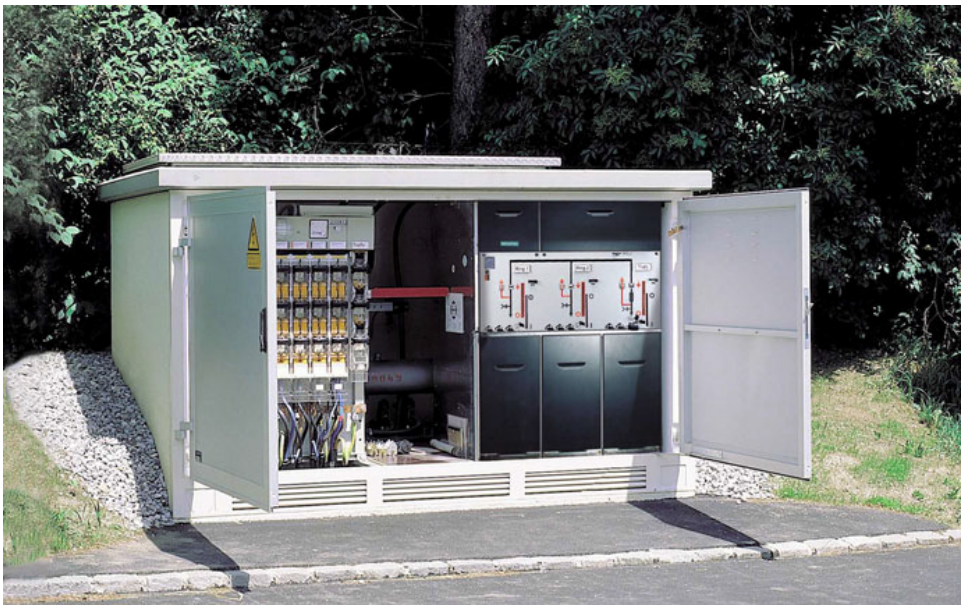

Figure 2.4: Transformer station by Siemens. Left: LV switches, right: MV switches and transformer [15]

the TSt consists of one operating and one reserve transformer both having the same rating and placed in the same station.
In certain areas, for example valleys in the mountains or elongated villages, it is sometimes preferred to place two (or more) TSts which operate in open-ring configuration along the areas longer axis.
As this project focuses on radial configuration in the low voltage level, it is the best choice to place the transformer at a location which minimizes the distance to all the connected nodes [15].

kVA rating Design and rating of transformers for distribution systems are in general subject to the particular conditions of the respective supplied area (construction type, rated apparent power, rated voltages, ...) but in order to have spare transformers and to provide cost efficient maintenance on the LV level the number of different types and ratings is kept limited [12]. The available transformer ratings (according to EN 50464 [18]) for different areal classes are listed in Table A.1. In all but the two very rural classes 630 kVA transformers are the most popular standard transformers in use.
Larger transformers would have enough power to supply more customers but due to the relatively low load density in German cities (compared to other industrialized countries) the voltage drop along the lines would violate the allowed power quality limits.
As public LV transformers generally exhibit less than 4500 full-load hours per year an economical operation is only possible by temporarily exceeding

the rated apparent power. Luckily time-periods of very high coincident grid demand and therewith the overloadings generally coincide with winter so that the transformers' lifetimes are not affected [12]. But literature values to the maximum overshoot over the rated power, by which the transformer approximately can be dimensioned, differ:

1. TSts with less than 3500 full-load hours can be sized according to IEC 60076-7: $\frac{S_{\max}}{S_r} = 150\%$ [19]
2. transformers can be loaded with up to 140% of its rated power [20]
3. $\frac{S_{\max}}{S_r} = 120\%$ [1]

For this project a compromise between the two smaller numbers is chosen, also because the households' peak loads were set to a relatively small number and to maintain a buffer for line losses. So transformers are dimensioned according to this condition:

$$S_r > \frac{S_{\max}}{1.3}. \tag{2.2}$$

In this formula $S_{\max}$ represents the maximum coincident load seen from the transformer node.
Using the maximum non-coincident load (the sum of the maximum loads $S_h = \frac{p_{pk,h}}{\lambda}$ of all n households) and a degree of simultaneous usage $g_\infty = 0.06$ the estimated coincident load $S_{\max}$ is [12]:

$$S_{\max} = (g_\infty + (1 - g_\infty) \cdot h_t^{-3/4}) \cdot \sum_{h=1}^{n} S_h \tag{2.3}$$

Where $g_{h_t} = g_\infty + (1 - g_\infty) \cdot h_t^{-3/4}$ returns the factor to calculate a single household's load share of the total coincident load of h_t connected households.
As it can be seen in Figure 2.5 distribution transformers are designed for maximum efficiency at 50% to 70% for the above explained reason of few full-load hours [13]. This observation can be used as a secondary criterion for sizing the transformer respectively in order to verify the sizing.

Connection The number of transformer terminals (feeders leaving the transformer) depends on the transformer model. The average and standard deviation of leaving feeders by ACl is listed in Table A.2.
The number of feeders leaving the TSt does not vary much because the transformers and lines have standard sizes, in urban areas the number of feeders ranges from 4 to 6 and in rural areas from 1 to 3 [1].

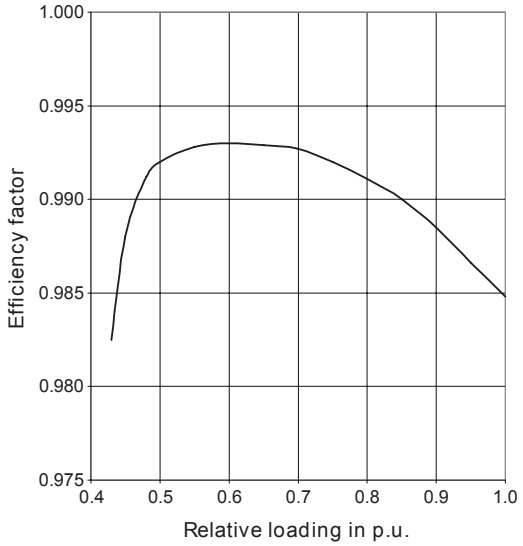

Figure 2.5: Efficiency curve of a LV transformer $S_r = 630\,\text{kVA}$ [12]

MV: Substations

For SSts in the primary distribution much less data than for TSts was available. One reason is that SSts come in a much higher diversity because they are built up modular (gas-insulated or air-insulated).
Designs and ratings vary over a large scale depending on the local load density, the number and the demand of connected MV consumers and the geographic conditions (75 MVA to 250 MVA in urban areas, 20 MVA to 200 MVA in rural areas).

Location In the model by Rui et al. a possible locations for the HV/MV-transformer SSt is either the center or the corner of the supply area [7]. For supply areas with relatively high load density the SSt is ideally placed centrally and supplies the TSt via open-ring configuration [15].
In this project different possibilities for the substation-placement are realized: (1) geographically centered between all loads (only TSts so far) (2) centered between loads by position and power demand (3) user defined position.

Rating As mentioned above, the rating of SSts and the number of installed transformers depends on the total demand.
The number of loads connected via TSts to one SSt can be very large so the coincidence is very low and the total load curve seen from the SSt is relatively flat. Therefore transformers in SSts operate most of the time at 100% of their rated power unlike TSts do [12]. Consequently the best way to calculate the approximate necessary rating of the SSt is by calculating

the total coincident load of all connected households h_s so that

$$S_r = h_s \cdot \frac{18\,\mathrm{kW}}{\lambda} \cdot (g_\infty + (1 - g_\infty) \cdot h_s^{-3/4}) \tag{2.4}$$

with power factor $\lambda = 0.9$ and coincidence factor $g_\infty = 0.06$.

Connection Post specifies a range of 5 to 30 connected TSts on each of the substation's outgoing rings, increasing with lower load density (from urban to rural) [21].
The maximum number of TSts per ring is limited to 64 in Germany [22].
The number of rings and terminals can be assumed to be unlimited in this project as substations are equipped with large bus-bars from where the ring feeders start off.

2.2.3 Lines

Power lines are the elements that connect the customer loads with the TSt respectively the TSts with the SSt to transport electric energy. Substations, transformers and distribution cabinets were explained in the previous Sections 2.1.3 and 2.2.2.
In compliance with the general situation in Germany (LV: 88% Cable, 12% OHL; MV: 78% Cable, 22% OHL) it can be assumed in this project that all lines are aluminum underground cables.
Service laterals, which connect the buildings to the feeders installed under the adjacent road are not considered in this project due to the lack of relevant data and the phasing of the cables will be neglected (as for the loads). Consequently each cable is defined by (1) the starting and ending point (2) the resulting distance and (3) the conductor size. (1) and (2) depend on the position of the loads and the routing (see Section 2.3), (3) is explained below:

Sizing of the lines

The following steps describe a procedure to determine the conductor cross-section based on the recommendation of a Swiss cable manufacturer [23]:

1. Calculating the nominal current

$$I_N = \frac{S_{\max}}{\sqrt{3} \cdot U} \tag{2.5}$$

   U = concatenated nominal voltage [kV]: LV 0.4 kV
   $S_{\max}$ = transmission power [kVA].

2. Determining correction factors for laying (underground either in tubing or directly in soil, overhead) and shield grounding. For standard conditions the correction factor equals 1.

3. Identification of the necessary cross-section using current carrying capacity tables.

4. Recheck the cross-section

   - **MV:** The short-circuit current must not exceeds the short circuit current capacity. If so a larger cross-section must be chosen:

     $$I_{SC} = \frac{S_{SC}}{\sqrt{3} \cdot U} \tag{2.6}$$

     S_{SC} = short-circuit power [kVA]

   - **LV:** The voltage drop along the line must not exceed the allowed maximum voltage drop. Otherwise a larger cross-section must be chosen.
     According to the European norm EN 50160, the maximum permissible voltage variation ΔU at the end customers' installations is limited to $\Delta U_{\max} < \pm 10\% \cdot U_N$ [24]. When the customers' installations are unknown a maximum voltage deviation of $5\% \cdot U_N$ at the service lateral is a sufficiently conservative approximation [12].
     The additional voltage drop occurring directly at the transformers primary side should be accounted with additional 2% resulting in a voltage drop limit of $3\% \cdot U_N$ for LV lines [13].

For the case of low voltage cables, this manufacturer provides a diagram of the optimal conductor cross section given a load moment and a permissible maximum voltage drop (Appendix C).
To illustrate calculation of the load moment their example is shown in Figure 2.6: One transformer feeds four different loads $P_1 = 8\,\text{kW}$, $P_2 = 11\,\text{kW}$, $P_3 = 30\,\text{kW}$, $P_4 = 15\,\text{kW}$ with one feeder. The cable-length between the loads is $L_1 = 90\,\text{m}$, $L_2 = 80\,\text{m}$, $L_3 = 110\,\text{m}$, $L_4 = 70\,\text{m}$.

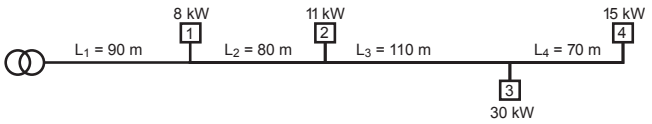

Figure 2.6: Example feeder for load moment calculation, total load moment 16 240 kW m

The total load moment is calculated by stepwise multiplying every load with

its distance to the transformer and summing these 4 load moments:

$$\begin{aligned} P_1 \cdot L_1 &= 720\,\text{kW m} \\ P_2 \cdot (L_1 + L_2) &= 1870\,\text{kW m} \\ P_3 \cdot (L_1 + L_2 + L_3) &= 8400\,\text{kW m} \\ P_4 \cdot (L_1 + L_2 + L_3 + L_4) &= 5250\,\text{kW m} \\ \text{total load moment} &= \mathbf{16240}\,\text{kW m} \end{aligned}$$

Based on Appendix C the adequate copper cross-section for $\Delta U < 3\%$ would be Cu=95 mm^2.

Line losses

Due to the lower voltage level in LV and MV networks the losses are much higher than in HV. They can be divided into three different types of losses: Ohmic losses, shielding losses and fuse losses.
For the commonly used copper shielded cables up to 250 mm^2 the ohmic losses are much larger than both shielding and fuse losses. Accordingly the latter two can be neglected in the loss calculation [23].
The ohmic losses are

$$P_l = I \cdot R \tag{2.7}$$

where $R = R_{20} \cdot (1 + \alpha(T - 20\,°\text{C}))$ and $\alpha = 0.00403$ (aluminum).
An approximation of line losses is not a task of this project but might be an interesting factor for later grid studies, therefore the ohmic resistance of the lines is calculated.

2.3 Power line routing

2.3.1 LV system

As discussed above, there a several different kinds of grid structures for the low voltage systems but because of their simple operation radial networks were and still are the most recommended structure. So this section covers the routing of cables of a *radial* LV grid.
For defining the supply area of a transformer and connecting the supplied loads by cable the following criteria have to be considered:

- **quality of power:** Reduce voltage variations
- **total costs:** Investment in large cable cross-section against higher operation costs by energy losses and aging of cables with smaller cross-section

- **reliability/redundancy:** Higher reliability means higher redundancy at higher costs. Trade-off between non-intermittent supply and larger investment for redundant technical devices. Three different reliability levels are presented in Section 2.1.4.

Both voltage drops and energy losses are proportional to the length of the line and inversely proportional to its cross-section which was covered in Section 2.2.3. To keep investment costs low and avoid laying of unnecessary line the minimum spanning tree algorithm, which minimizes the total length of all the low voltage grid's cables, can be used.

Minimum spanning tree

The MST algorithm takes a connected undirected graph as input and returns a tree which connects all the graphs' vertices with the shortest possible total line length and without any cycles.
O. Borůvka was the first to formulate and solve the MST problem in 1926 [25] while working on power grids. Several newer papers on distribution system design e.g. [26] recommend the MST to initialize a radial network configuration.
The popular MST solution by R. Prim is presented in Algorithm 1 [27].

Algorithm 1: Prim's MST algorithm

Data: Connected weighted (e.g. edge length) graph with vertices V and edges E
Result: V_{MST} and E_{MST} of MST
$V_{\mathrm{MST}} = x$, x is arbitrary vertex from V (root of tree), $E_{\mathrm{MST}} =$;
while $V_{\mathrm{MST}} \subset V$ **do**
  For $u \in V_{\mathrm{MST}}$ and $(v \in V) \notin V_{\mathrm{MST}}$ choose an edge u, v with minimal weight;
  Add v to V_{MST}, and u, v to E_{MST};
end

Cluster analysis k-means

The voltage drop can not only be avoided by taking the shortest possible path to the load but also by reducing the direct distance between the consuming load and the supplying transformer. For an area which has to be supplied by more than one TSt cluster analysis can be used to determine the supplied area of each TSt.
The k-means algorithm partitions n observations into k clusters so that each observation belongs to the cluster with the nearest centroid. The cluster's centroid is the point to which the sum of distances from all objects in that

cluster is minimized (for advantages and limitations see [28]).
In our case, the consuming loads are the n observations, the total number of low voltage grids equals the number of clusters k and the centroid location can be used as the ideal location for placing the TSt.

2.3.2 MV system

For the medium voltage grid the same criteria as for LV grids should be considered: Quality of power, total costs and reliability. But for the medium voltage level a cost minimizing *open-ring* configuration is the structure of choice due to higher reliability requirements.
As for low voltage, costs are approximately proportional to the total line length so the problem becomes connecting all transformer stations to the substations in rings of minimum total line length.
For the case of one single ring and one substation the problem equals the *travelling salesman problem (TSP)* and the same solution algorithms can be used.

Vehicle routing problem

Two constraints interfere with the TSP approach: (1) keeping the distance between TSt and SSt short in order to minimize voltage drops and (2) complying with maximum number of TSts a ring-feeder can supply. To include these two constraints it can be necessary to feed the TSts via different rings from the substations.
Allowing multiple rings (and substations) leads to the *vehicle routing problem (VRP)* (with multiple depots). Bozic and Hobson provide an overview of different approaches to these problems [29].
In this project we assume that one single SSt feeds the transformer stations via different feeders where all feeders originate and terminate in the same SSt so that the problem can be solved with standard VRP algorithms.

Sectioning of the ring

The MV grids in this project are operated in open-ring configuration. In order to guarantee reliable operation of the grid all line sections are equipped with disconnectors so that faulty TSt can be disconnected while maintaining the supply for all the other TSts.
This set-up also demands a default sectioning point for normal operation. In this project the line which balances the sums of maximum demands on both half-rings is chosen as sectioning point.
Other possibilities would be balancing (1) the sum of the transformer ratings or (2) the total length of the half-rings.

Chapter 3

Implementation

In this chapter, the MATLAB-implementation of the module and its control are explained. As in this project the grid generation is based on a spatial population density map a graphical interface provides the user with the layout of the grid and displaying options. The data structures which describe the grid are returned to the user in matrices.
The module is invoked in MATLAB with the command

$$[\text{LV\_CP, LV\_L, MV\_CP, MV\_L, TD, S}] = \textit{grid\_builder\_main\_GUI} \quad (3.1)$$

with a variable number of outputs, namely low voltage connection points LV_CP, low voltage lines LV_L, medium voltage connection points MV_CP, medium voltage lines MV_L, the data from the GUI table TD and further statistics S.

3.1 Data

3.1.1 Input

In this MATLAB implementation two types of input parameters are used. Fixed constants which are defined in *fixed_parameter.m* (Table D.1) and the parameters loaded from the file *user_parameters.m*. The user is advised to only adjust the latter ones which are listed together with their default values in Table D.2.
In addition to the pre-defined parameters the user has to choose between different construction options during the construction procedure. The different options offered in these dialogs are summarized in Table 3.1.

3.1.2 Output

The information and properties of the distribution grid's components are stored in matrices and returned to the user for further evaluation after finishing the construction of the distribution system model.

Low voltage connection points

For each independent low voltage grid both transformers and loads are stored together in a nodes-matrix and all these matrices of the independent grids are put into the cell array LV_CP.

Transformers In the first line(s) of the grid matrix the transformer(s) are described by position x_t and y_t, the rated power S_r [kV A], the total number of households connected to the transformer h_{Sg}, the maximum coincident apparent power demand $S_{\max}$ [kV A], the yearly energy supply E_{Sg} [kWh] and the index of the sub-grid the transformer supplies Sg (see Section 3.3.2) in the following order:

$$[x_t \; y_t \; h_{Sg} \; S_{\max} \; E_{Sg} \; S_r \; \mathrm{Sg}]$$

As the number of independent LV systems is user-defined, it can occur that the maximum available transformer rating is not high enough to supply all loads in the specific system so it gets split up into multiple interconnected sub-grids (Section 3.3.2). For this reason one LV system can have more than one transformer.

Loads In the following lines of the matrix all system's consumers are defined. Each row contains the position of a building's connection to the feeder x_{cp} and y_{cp}, the number of households per building h_{cp}, the buildings coincident peak power demand at the connection point p_{pk} [kW] the buildings yearly energy consumption E_{cp} [kWh], the ACl of the pixel D_{px} where it is placed and the index of the sub-grid Sg, it belongs to:

$$[x_{cp} \; y_{cp} \; h_{cp} \; p_{cp} \; E_{cp} \; D_{px} \; \mathrm{Sg}]$$

The buildings coincident peak load is only relevant for cable sizing. For transformer dimensioning the total peak load is different from the sum of the buildings peak loads because (1) of a higher coincidence factor and (2) because of the line losses.

Differentiation To allow an easy differentiation of transformers and loads yearly consumption is stored with a negative sign while the supply by the transformer is positive (5^{th} column).

Low voltage lines

The information about the connecting lines is stored row-wise in a line-matrix for each independent low voltage grid. This approach was preferred to the use of adjacency matrices because it eases handling each line as an object. The relevant information about each line are the cable length l [km],

the start-node n_s and the end-node n_e (corresponding to the row in the node-matrix), the index of the sub-grid it belongs to Sg, the cross-section of the line c, the ohmic resistance (operating temperature 50 °C) of the line R [Ω] and their current operation state St (open/closed: 0/1):

$$[l\ n_s\ n_e\ \mathrm{Sg}\ \mathrm{Sg}\ c\ R\ \mathrm{St}]$$

The open lines which are interconnecting possible sub-grids are stored below the closed lines. For the closed lines both the start sub-grid Sg_s and the end sub-grid Sg_e are given:

$$[l\ n_s\ n_e\ \mathrm{Sg}_s\ \mathrm{Sg}_e\ c\ R]$$

As for the nodes one matrix contains all the lines of one independent distribution grid. The line matrices of different independent grids are organized in the cell array LV_L.

Medium voltage connection points

This project assumes that one single SSt supplies the whole grid. Accordingly this SSt is described in the first row of the matrix MV_CP by its position x_s and y_s, S_r the recommended rating according to Equation (2.4), the sum of the maximum coincident power demands of the transformers $S_{\max}$, the total number of households in the LV grid and the total yearly consumption E_s [MWh]:

$$[x_s\ y_s\ h_s\ S_{\max}\ E_s\ S_r]$$

The TSts from the LV grids become loads in the MV grid and are listed below the SSt. The relevant information about these TSts are the position x_t and y_t, their maximum power demand $S_{\max}$, the number of households in the LV grid h_t, the yearly consumption E_t [MWh] and the Ring Rg they are connected to:

$$[x_t\ y_t\ h_t\ S_{\max}\ E_t\ \mathrm{Rg}]$$

Medium voltage lines

The lines in the medium voltage (Matrix MV_L) have the same specifications as the LV lines except for two changes: Instead of the index of a sub-grid the index of the ring Rg by which the load is supplied is given and furthermore the operating state St (open/closed: 0/1) of the line is indicated:

$$[l\ n_s\ n_e\ \mathrm{Rg}\ c\ R\ \mathrm{St}]$$

Statistics

The statistics matrix S returns for each available low voltage cross section (row 1 to 9), medium voltage cross section (row 10 to 15) and transformer rating (row 16 to 21) its absolute (second column) and relative usage (third column). The absolute usage of the cross sections is measured in km of lines but for the transformer ratings in deployed transformer stations. The relative usage consequently is given in percent and calculated in relation to the overall line length respectively to the overall number of transformer stations.

Unit system

During project development the idea of using p.u. units instead of SI units was considered. Whilst the p.u. system is very useful for the qualitative analysis of an active power system (easier detection of gross errors, overloading, ...) the SI units seemed to be more suitable as grid characteristics are generally provided in SI units, as the necessary calculations are limited to the dimensioning of lines and transformers and because no grid analysis (neither steady state nor transient) is performed.
On the contrary the p.u. system would require a double conversion: The initially given input parameters first have to be converted to p.u. for the grid construction but for comparison to literature they have to be in SI units again.
Hence SI units are used throughout the project.

3.2 Graphical user interface

As visualization is very important in this project for drawing the spatial map and the grid layout a graphical user interface is provided for generating the distribution systems. The main GUI was created in the MATLAB-GUIDE environment and is shown in Figure 3.1.
Each of the GUI's elements (listed below) invokes different functions (so called callback routines) when constructed/clicked/deleted. The other elements' *addresses* are passed along these callbacks via the *handles*-structure provided by the GUIDE environment.
In this software the *handles*-structure is also used to pass variables and matrices between the different callbacks.
The most important part of the GUI is the chart in the middle in which spatial map, connection points and lines are drawn (1). Below the chart a table lists characteristic information about the project for both voltage levels (2). Above it a toolbar with push buttons for basic chart control is placed (3). At the top of the GUI the menu bar allows further control possibilities in the two drop-down menus *Project* and *Show* (4).

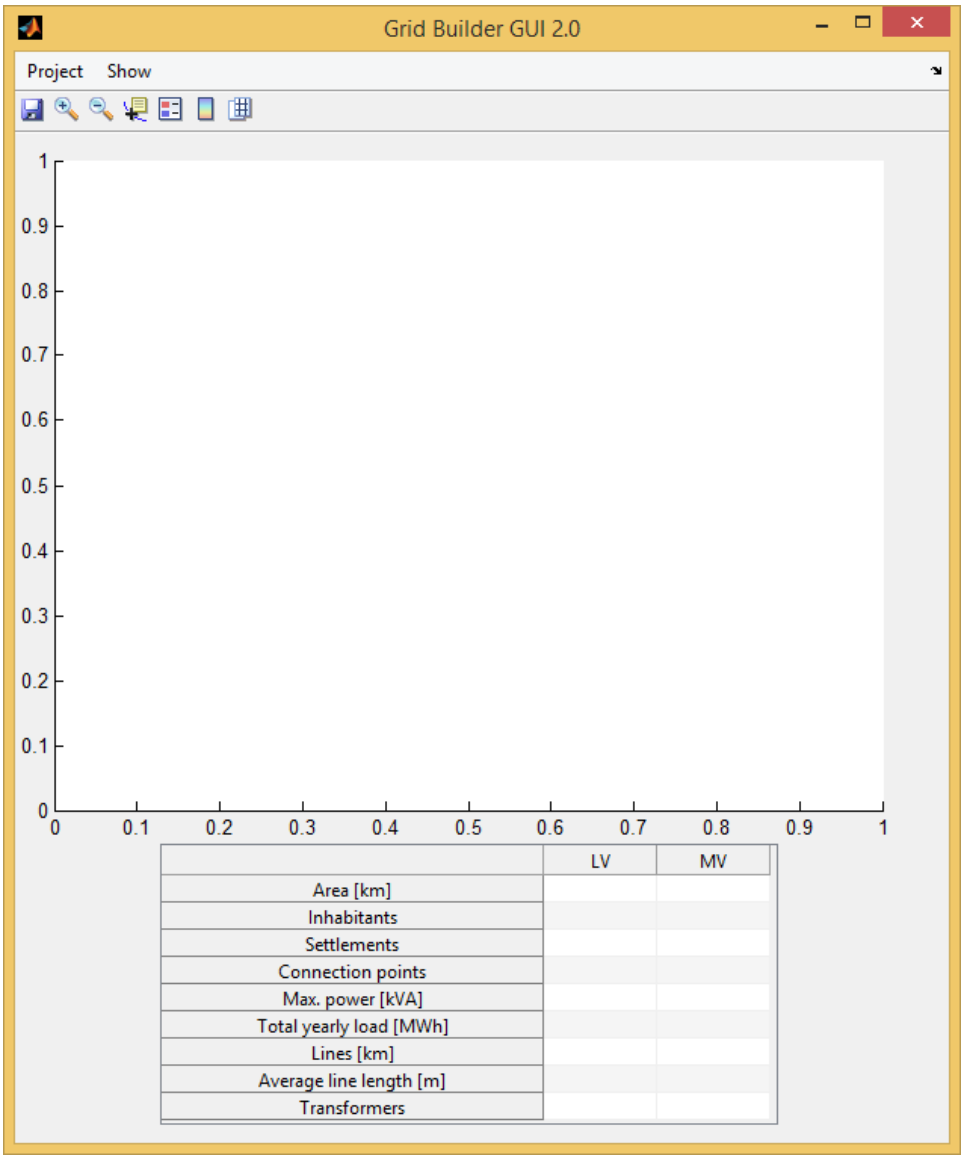

Figure 3.1: Graphical user interface

3.2.1 Chart

The chart covers the largest part of the GUI and default it blank and scaled to 1×1 km^2.
The chart's size is linked to the size of the GUI so resizing the GUI directly affects the size of the chart.

3.2.2 Table

In the table the most relevant characteristics of the grid are updated dynamically during the construction phase. For both voltage levels the following properties are listed:

- Area [km]
- Inhabitants
- Settlements
- Connected loads
- Maximum power [kVA]
- Yearly consumption [MWh]
- Lines [km]
- Average CP distance [m]
- Transformers
- Installed power [MVA]

3.2.3 Toolbar

Seven pushbuttons which are placed above the chart area allow quick basic control over the chart. The Menu *Show* offers further possibilities to adjust the presentation of the distribution system area:

button	function
save	same as *Save Project* (Menu bar)
zoom in	zoom in by a factor of 2 with each mouse click
zoom out	zooms out by a factor of 2 up to original size
datacursor	show exact coordinates of a selected datapoint
colorbar	display/hide the color legend on the right of the chart
legend	display/hide the line and CP legend
grid	display/hide grid lines on the charts top layer

3.2.4 Menu bar

The menu bar offers two drop-down menus *Project* and *Show*. The first one provides the basic start and save routine to initialize and end the project whilst the latter one contains tools to improve the network visualization.

Project	function
New Project	Initializes the construction of a distribution grid
Save Project	Allows saving the output data as (*.mat*) and the grid map (*.fig*) to a personal folder via a dialog box
Show	shown/hidden objects
Pop Centers	Placed population centers and their labels
Density map	Density heatmap
LV Loads	position of buildings
MV Loads	position of the TSts
LV grid	active and open lines of the low voltage grid & TSts
MV grid	active and open lines of the medium voltage grid & SSt

Initially it was intended to give the user the possibility to pause, save and exit his current project at every dialog and to reload the saved data and continue the project later. For this reason all steps described below are embedded in a large switching-routine which allows an easy resumption with a known case-number.
The save-open-concept was dropped at a later development stage when it became clear that the program works without computationally intensive algorithms but some artifacts of the concept remained in the code, e.g. an *open*-callback and the switching routine.

3.3 Generation of a distribution grid

In this section the distribution grid generation procedure is explained. The procedure is initialized by starting a new project from the menu bar *Project* → *New Project*. The procedure is illustrated in Appendix D.3.

3.3.1 Modeling of a spatial load map

First an input dialog asks the user for the total area and inhabitants of the distribution system. Then he is given the possibility to place population centers of different densities and size on a discrete quadratic map with a user-defined resolution (default 100×100 pixel).
Subsequently the user chooses a smoothing factor for the map in order to reduce the gradients between the different population centers.
Based upon the pixels' population density the ACl and the number and type of connected building is determined for each pixel. In the next step the buildings are randomly distributed within the pixels and their electricity consumption is chosen according to Section 2.2.1.

1. An Input dialog demands area A and number of inhabitants I

2. The map is discretized into 100×100 quadratic pixels each of size $\frac{A}{10000}$

3. The user chooses the background density from 8 different densities.

   - zero
   - far-scattered ($\widehat{=}$R1)
   - scattered ($\widehat{=}$R2)
   - slightly scattered ($\widehat{=}$U1)
   - fairly populated ($\widehat{=}$U2)
   - slightly dense ($\widehat{=}$A1)
   - dense ($\widehat{=}$A2)
   - very dense ($\widehat{=}$A3)

   These densities have to be seen relatively to (1) the total population density given through I and A and (2) the density of the population centers placed in the subsequent step. Nonetheless the pixels' values are set to a density drawn randomly from between the limits of the areal class corresponding to the chosen relative density.
   The map's background takes on the color of the chosen background density.

4. For each of the 8 densities the user can place c quadratic settlement centers on the map which are immediately plotted in their color.
   The densities are defined the same way as they are in the second step, for each center there is one random draw of its density. The centers' sizes increases with density, for *zero* it is one pixel, for *very dense* the center extends 7 pixel in every direction to a total area of $15 \times 15 = 225$ pixels.
   The population centers' midpoints and areas are plotted into the map.

5. The user defines the smoothing out of the map on a scale from 0 to 100 either via input field or by moving a slider with the mouse. He can directly see the effect of the smoothing in the map before he confirms his choice. The higher the smoothing factor is set the more the quadratic centers become circular and larger.
   The used smoothing function *smooth2a.m* smoothes the data in a matrix M using a mean filter over a rectangle of the size $(2s_x + 1) \times (2s_y + 1)$. It works like a two dimensional moving average where the value of the elements of the rectangle with center i is replaced by the rectangle's mean value. It was developed by G. Reeves [30].
   Several tests revealed that the best graphical results are achieved with a rectangle of size 3×3 ($s_x = 1,\ s_y = 1$) repeated up to 100 times (maximum resolution).

6. The smoothed map is linearly scaled up to meet the total number of inhabitants I.
   The population I_{px} and the density D_{px} of each pixel is calculated, so

that the areal classes of the pixels ACl_{px} are defined.
Knowing the average number of households per connection point of each areal class (Table A.4) the software calculates the number of connected buildings in each pixel $N_{cp,px}$.

7. Using the density class C_{px} and the number of buildings $N_{cp,px}$ the software defines the connection points:
   (a) For each connection point CP_i its x and y coordinates are drawn from an uniform distribution to randomly position the building within the pixel
   (b) The number of households in each building is drawn from the uniform distribution over the range of households as given in Table 2.3.
   (c) The yearly load of each building is the product of the average yearly load of a household of the corresponding class (Table 2.3) and the number of households per building h_{cp}.
8. The loads are plotted as black cross-marks onto the colored spatial map.

The design of the spatial map and the smoothing effects are illustrated in Figures D.2 and D.3

3.3.2 Generation of the LV distribution grid

Clustering of low voltage systems

After the loads are plotted, the user has the possibility to set the number of independent (not interconnected) low voltage distribution grids. As default

$$G_{\mathrm{rec}} = \frac{g_{h_s} \cdot h_s \cdot 18\,\mathrm{kW}}{\lambda \cdot 630\,\mathrm{kVA} \cdot 1.3} \tag{3.2}$$

grids are recommended. G_{rec} is calculated from the systems total coincident consumer peak load divided by the maximum permissible transformer power. Furthermore the software proposes a minimum and maximum number of grids calculated from the number of placed centers c, the number of of connection points connected to the feeders CPs_t and the maximum number of connection points per transformer $\mathrm{CPs}_{\mathrm{max}}$:

$$G_{\mathrm{rec,min}} = max\left(1, min\left(c, \left\lfloor \frac{\mathrm{CPs}_t}{\mathrm{CPs}_{\mathrm{max}}} \right\rfloor\right)\right) \tag{3.3}$$

$$G_{\mathrm{rec,max}} = max\left(c, \left\lfloor \frac{\mathrm{CPs}_t}{\mathrm{CPs}_{\mathrm{max}}} \right\rfloor\right) \tag{3.4}$$

If the default value does not lie within these boundaries, it is to be adjusted to the closer one.

The user can ignore these recommendations and chose an arbitrary number of independent low voltage grids g.
In order to divide the area geographically k-means clustering is applied on all loads with k = g. For the resulting clusters the maximum linear distance and the maximum average distance is returned to the user so that he can increase or decrease g to initialize another run of k-means until he confirms his choice.
Finally, the identified centroid positions of each of the clusters are stored as the grids' transformer locations and for each independent low voltage system the loads and transformers are sorted into a matrix as described in Section 3.1.2.
The clustering dialogs and effects are illustrated in Figure D.4.

Connecting the LV components

For each of the independent low voltage systems G_i, $i \in 1 \dots g$, the following steps are implemented to connect the consumer loads to the TSts:

1. **Necessary Sub-grids:** If the load clusters do not fulfill the conditions to ensure supply k-means clustering is executed on the grid G_i with increasing k until the conditions are met. This way G_i is split up into sg = k interconnectable sub-grids. The conditions are:

   - The largest of the available[1] transformers (Table A.1) must be large enough to approximately supply all h_t households in G_i. The conditions approximates line losses with 5% of the coincident power:
   $$\mathbf{1.25} \cdot 630\,\mathrm{kVA} > g_{h_t} \cdot h_t \cdot \frac{18\,\mathrm{kW}}{\lambda}$$
   - The longest direct distance $d_{t,\mathrm{cp}}$ from the transformer to any load is shorter than the maximum distance allowed $d_{\max}$(= 700 m).
   $$\max_{\mathrm{cp} \in \mathrm{CPs}} d_{t,\mathrm{cp}} < d_{\max}$$

   When both criteria are fulfilled the node-matrix is updated by the position and number of transformers (centroids) and the loads' sub-grid indices SG_j resulting from the above clustering.

2. **Distance Matrix:** The distance matrix of the nodes (transformers and all buildings) D_i is calculated. The distances can either be calculated in Euclidean (default) or cityblock metric (see Section 4.3.3).

3. **Minimum spanning tree:** For each sub-grid SG_j the MST starting at the transformer $t_{i,j}$ is calculated.

[1] The average of the loads' pixel ACl ACl_{px} gives the sub-grid's areal class ACl_{Sg}

The MST implementation is based on Prim's algorithm but modified with regard to the number of transformer outlets:
Based on the average ACl of the appendant loads the number of transformer outlets O_T is drawn from a normal distribution according to Table A.2. The O_T closest loads are directly connected to the transformer and subsequently the minimum spanning tree is initialized starting from these $O_T + 1$ fixed nodes. The resulting lines are then stored in matrices as described in Section 3.1.2
For each connection point m its degree $a(m)$ (adjacent nodes) is stored:

- $a(m) = 1$: end point
- $a(m) = 2$: normal node
- $a(m) > 2$: junction[2]

4. **Interconnection of Sub-grids:** The user sets the maximum number of interconnections of each sub-grid to other sub-grids l_{SgSg} through an input dialog once.
   For each sub-grid SG_j the $\mathrm{l}_{j\mathrm{Sg}} = \min(l_{\mathrm{SgSg}}, \mathrm{sg})$ shortest connections to the other sg sub-grids $SG_{k,k\neq j}$ are searched and stored as an open line. To avoid repetitions the algorithm checks for already existing connections between k and j.

5. **Dimensioning the transformer:** As default the transformers are dimensioned sub-grid-wise as described in Section 2.2.2 for the maximum coincident load $S_{\max}$. $S_{\max}$ is approximately calculated from the total number of supplied households and the coincidence factor.
   Then the density class specific transformers are compared to $S_{\max}$ and the lowest rating fulfilling Equation (2.2) is chosen.
   The user can also choose a second option for dimensioning in the set-up: All transformers of interconnected sub-grids are rated with the same power as the largest necessary transformer so that each transformer can replace another one in case of an outage.

6. **Dimensioning the lines:** To initialize the calculation of the lines' cross-sections the end nodes ($a = 1$) of the grids are searched. Then a recursive search for each nodes parent is performed. Thereby the parent's children cumulative load moment and their cumulative load is stored in the parent's data and based on these, the cross-section and the according resistance of the line is determined as described in Section 2.2.3.
   At a junction, the recursion is paused until all the children of the junction node have been evaluated. This is done by a second degree-index for each node which is reduced by 1 if an appendant line is dimensioned and recursion is only possible if this index equals 1.

[2]Real loads are not placed directly at junctions/cabinets but within meters distance.

In case the sub-grids are interconnected the interconnecting line element connecting two sub-grids l, m are dimensioned by an approximated load moment

$$\text{loadmoment} = \min_{k \in [l,m]} S_{\max,k} \cdot \text{dist}(i,j) \tag{3.5}$$

resulting from the maximum coincident power demand (Equation (2.3)) at the smaller of the two transformers times their line distance.
Then recursively all line element between the connection points of the open line and the TSts are sized accordingly.

7. **Plotting the network:** The sub-grids' power line structure is plotted into the map as black straight lines. The open interconnections between the sub-grids are shown as dotted red lines. The TSts are plotted as yellow circles.

The LV grid design steps are shown in Appendix D.5.

3.3.3 Generation of the MV distribution grid

As described in Section 2.3.2 one single SSt supplies all existing TSt. Accordingly the following steps only have to executed once:

1. **MV matrix:** Iteratively the relevant TSts' data is extracted from the LV matrices and stored in the MV matrix.
The total number of households in the network, the total yearly energy consumption and the sum of the TSts' maximum demands are stored in the first row of the MV matrix. The substation rating is calculated according to Equation 2.4.

2. **Placement of the substation:** Via dialog box (Appendix D.6) the user can choose between four different options to place the substation:

   - by mouse-click
   - geographic center of the map
   - geographic mean of the TSt
   - geographic mean of the TSt weighted with their maximum loading

   The (calculated) substation's position is saved in the MV node-matrix.

3. **Identifying the ring configuration:** The user-set parameter for the maximum number of TSt per ring $\mathrm{T}_{\mathrm{rg,max}}$ defines the number of rings:

$$n_{\mathrm{rg}} = \left\lceil \frac{n_{\mathrm{T}}}{\mathrm{T}_{\mathrm{rg,max}}} \right\rceil \tag{3.6}$$

The user is offered the option to balance the number of TSts per feeder. If activated the new maximum number of permissible TSts is set to

$$\mathrm{T}^{*}_{\mathrm{rg,max}} = \left\lceil \frac{n_{\mathrm{T}}}{n_{\mathrm{rg}}} \right\rceil \tag{3.7}$$

In practice reducing $\mathrm{T}_{\mathrm{rg,max}}$ *may corrupt the minimization of the total line length. Together with this project's non-optimal Vehicle Routing implementation the default constraint will result in one ring which is distinctly smaller (less TSts) than all other rings, the balanced constraint on the other hand leads to rings of same size (equal number of TSts).*

4. **Vehicle routing problem:** After calculating the distance matrix from the TSts' and the SSt's positions the VRP algorithm is executed. In this module's version a VRP script (Algorithm 2) based on the

Algorithm 2: VRP nearest neighbor

Data: Distances $D_{s,e}$ between TSts (and the SSt), $T_{\max}$ maximum number of TSts per ring
Result: n_{rg} Matrices each containing start and end nodes and length of all line elements of the rings

$\mathrm{T}_{\mathrm{unconn}} \leftarrow [\mathrm{TS}_1 \dots \mathrm{TS}_{n_{\mathrm{T}}}]$;
$n_{\mathrm{rg}} \leftarrow \left\lceil \frac{\#\mathrm{T}_{\mathrm{unconn}}}{T_{\max}} \right\rceil$;
for $r \leftarrow 1$ **to** n_{rg} **do**
  $s \leftarrow$ SSt;
  while $\#\mathrm{T}_{\mathrm{unconn}} > 0$ *&* $\mathrm{lines}(r) < T_{\max} + 1$ **do**
    find closest e in $D_{s,e}$;
    store line $\mathrm{l}_{s,e}$;
    $s \leftarrow e$;
  end
  find and store line $\mathrm{l}_{s,\mathrm{SSt}}$;
end

nearest neighbor algorithm is implemented. The algorithm is very quick but does not achieve an optimal solution. More sophisticated algorithms might be implemented in later versions (see section 4.4.3).

5. **Dimensioning the lines:** The necessary cross section for the lines is calculated ring-wise. For each ring the total coincident load momentum (based on the TSts's maximum coincident power demands) is calculated from both sides of the ring assuming the opposite connection to the substation to be open. Then the cross-section matching both this maximum coincident load and the user-given voltage drop

limit is stored for all line elements.
The resistance of each line element is calculated and stored.

6. **Locating the sectioning point:** As described in Section 2.3.2 several possibilities to open the ring exist. The user can choose between balancing by (1) transformer ratings (2) line length or (3) peak demand (households).
In all three cases ring-wise matrix calculations are performed to minimize the difference between both half-rings. For (1) and (3) the respective transformer properties $f(\cdot)$ are relevant so the last transformer t on the half-ring before the separation is identified by:

$$\min_{t\in 1\dots n_t-1}\left\|\sum_{j=1}^{t} f(j)-\sum_{j=t+1}^{n_t} f(j)\right\| = \min_{t\in 1\dots n_t-1}\left\|2\sum_{j=1}^{t} f(j)-\sum_{j=1}^{n_t} f(j)\right\| \tag{3.8}$$

For the lines-criterion (2) the line element l_{i+1} which will be disconnected must not be included:

$$\min_{i\in 1\dots n_l-2}\left\|\sum_{j=1}^{i} l_j-\sum_{j=i+2}^{n_l} l_j\right\| = \min_{i\in 1\dots n_l-2}\left\|2\sum_{j=1}^{i} l_j-\sum_{j=1}^{n_l} l_j+l_i\right\| \tag{3.9}$$

The above optimizations are only applied for rings with at least 3 connected transformers (4 lines). In the case of only one TSt the first of the two identical connections is activated, in the case of two TSts the line connecting the two transformers is disconnected.

7. **Plotting the network:** The MV lines are plotted similar to the LV lines but thicker. The SSt is plotted as a green circle.

Table 3.1: Overview of user dialogs

Dialog	**User input**
Grid area	Define area [km^2] and population
Population Map	Choose density levels (Section 3.3.1) for · Background density · Population centers
Smoothing	Set smoothing factor for the map (0 to 100)
LV grids	Set number of independent low voltage grids
LV voltage drop	Define voltage drop maximum (1% to 7%)
Interconnections	Set number of interconnections between sub-grids
Transformer rating	Set transformer rating calculation method so that it can fully supply · Its own Sub-grid · The largest connectible Sub-grid
Substation placement	Choose placement method · calculation - center of map - geographic center of TSts - rating-weighted center of TSts · mouse
Units per Ring	Decide allocation of TSts to Rings · maximum: fill rings up to maximum · balanced: balance TSts per ring
MV voltage drop	Define voltage drop maximum (1% to 7%)
Ring sectioning	Set ring sectioning method. Calculate sectioning point by balancing half-rings' · TS rating · TS peak loading

Chapter 4

Results and discussion

In this chapter the (1) load map, (2) LV distribution system and (3) MV distribution system outputs and layouts resulting from different testing sets are evaluated and the characteristics are compared to literature and reference data. Furthermore the measured computation time of each of the three main steps is discussed shortly and improvement potential regarding the software functionality is discussed.
The functionality of the module was tested with very basic map set-ups consisting of one single center of the same density as the background only scaled with regard to population and area. This is necessary to avoid differences in the testing spatial maps originating from the design procedure which does not yet allow the identical reproduction of more complex spatial maps.

4.1 Testing device

All computation time measurements were performed on the following device:

Device	Lenovo X220
Processor	Intel i7-2620M 2.7 GHz Quad-core
Memory	16 GB DDR3-RAM
Hard drive	256 GB mini PCIe SSD
Operating System	Windows 8.1 Pro 64bit
MATLAB	R2014a 64bit

4.2 Spatial load map

The construction of the spatial load map was inspired by the JavaScript heatmap script by P. Wied [31].
As the implementation of a dynamically evolving heatmap by continuous cursor querying and simultaneous plotting of the resulting map into Matlab

was assessed as exorbitantly time consuming (more than one week) the simpler approach of stepwise center-placement was chosen.
The load map design procedure is described in Section 3.3.1. As no other software of similar functionality is known the procedure and the results are assessed only qualitatively.
During software testing different observations on the behavior of this procedure were made which are outlined in the following section.

4.2.1 Results

Construction of the map

The implemented design procedure controls allow the construction of sketchy population density maps. Although it is quite difficult in the beginning routine may enable the user to draw precise density maps (see also Section 4.2.3). For distribution systems of realistic scale (at least one large transformer fully loaded, >1000 inhabitants, see Table 4.1) the different ACl of the pixels affect the randomized positioning of loads sufficiently so that different load densities are visible to the naked eye.

Table 4.1: Maximum number of households and inhabitants supplied by a standard transformer

S_r [kVA]	hh	inh.
50	20	40
100	64	129
160	121	244
250	211	426
400	364	735
630	604	1220

Connection points

The DSOs's database has an average of 1.95 persons per LV CP. As this number also includes commercial and industrial CPs the general validity of both the assumption of 2.02 persons per household (German governmental statistics) and the resulting density of CPs can neither be rejected nor confirmed.
In order to evaluate the connection point density a test map with 100000 inhabitants was designed for each ACl (the area was set to match the ACl's average population density, see Appendix A.3). The resulting CP density is compared to the DSO dataset density in Table 4.2.
We observe that the test results behave antitonically and differ strongly from the monotonically increasing reference values. But surprisingly a strong

Table 4.2: Comparison of CP density from DSO database and software results

	R1	R2	U1	U2	A1	A2	A3
reference CP density [/km^2]	42	68	95	122	147	216	613
test CP density [/km^2]	19	31	58	12	13	32	12
test household density [/km^2]	29	61	86	104	132	193	526

compliance of the tests' household density and the reference CP density exists.
This is either explained by a relative increase of non-private connection points (bureaus and commerce buildings) inversely proportional to the relative change of the CP density or by non-precise information in [17] and [2] about the collective usage of service laterals and CPs of row- and apartment buildings.

4.2.2 Load computation time

After the density map design the calculation of the pixels' ACls and the number of buildings on each pixel follows before these buildings' positions and number of households are drawn from random distributions.
In two test series with an increasing number of inhabitants (logarithmic: 1, 5, 10, ..., 500000, 1000000) on maps of 1 km^2 respectively 100 km^2 the load computation time was measured for the basic case of *very scattered* background and one single *very scattered* population center in the center of the map. Independent of the number of inhabitants the computation time commuted between 0.68 s to 0.77 s around a mean of 0.74 s.
For maps with more than one population center with a density different from the background density higher computation times up to 1.4 s were observed (e.g. for the map in Appendix D.3: 1.34 s).
For both the standard case and the case with a high population and many different centers the computation time is short and does not demand the users patience.

4.2.3 Scope for improvement

Relative density colors vs real density colors

Observation For a small number of population centers the population-corrected background density color may differ considerably in color from the originally chosen background density (Figure 4.1).

Explanation The reason is obvious, an example: The relative background density is set to *scattered* but the user-defined area and inhabitants result in

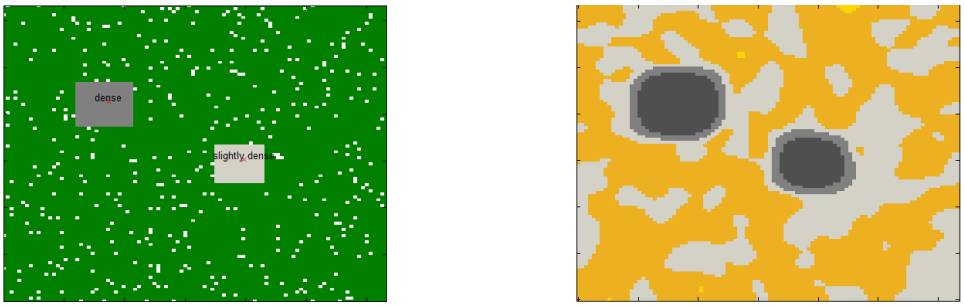

Figure 4.1: Density map before (left) and after (right) smoothing and scaling. Area 10 km^2, inhabitants 3000, smoothing factor 10

an average of 800 inhabitants/km^2 so the background is scaled up to areal class A3 (light green becomes dark gray).

Possible solution This problem could be avoided by choosing different colormaps for each the relative densities during the construction phase and the real densities resulting from the smoothing.
Furthermore the real densities could be illustrated with a color gradient within each class.
Another possibility is to allow the user to choose between two different color maps (1) the nine class-colors or (2) a high resolution gradient of population densities.
A thoughtful user will be able to use this software without getting confused by the mapping of colors during these two phases of the spatial map design. Therefore modifying the colormap is of low priority only.

Hidden effect of smoothing

Observation For a high overall population density (above A3) the does not see effects of the smoothing as the whole map is painted in the same color even if different population centers densities and a low background density was chosen as illustrated in Figure 4.2

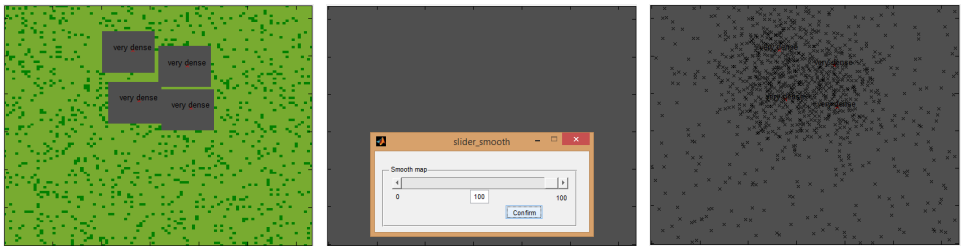

Figure 4.2: Hidden effect of smoothing (10 km^2, 100000 inh.): center placement (left), smoothing (middle), CP distribution (right)

Therefore the user gets the impression that changing the smoothing has no impact on the spatial densities.

Explanation The areal class A3 covers all population densities above $500\frac{\text{inhabitants}}{\text{km}^2}$ so for a high enough average population density all pixels (even the *very scattered* ones) of the map are scaled up to ACl A3 and accordingly the whole map appears dark gray for all smoothing levels.
Nevertheless the pixels do have different population densities based on the ratio between their relative densities chosen during map design.
A high smoothing factor flattens these differences out while a low smoothing factors leaves them more untouched.
In any case differences in the densities become visible through the positioning of loads which are shown after confirmation of the smoothing.

Possible Solution As for Problem 4.2.3 the easiest solution is introducing a color gradient within each areal class.
The user has no possibility to find the effects of the smoothing factor but by guessing and testing so the implementation of this solution is of high importance.

Decreasing building density with increasing areal class

Observation The density of connection points decreases in large steps between some ACls while the population density increases. Especially between the classes A2 and A3 the phenomenon is eye-striking (as in Figure D.5).

Explanation This observation may come surprising at first glance but is logically explained by the class specific average of housing units per connected building (Table A.4) which is not proportional to the increase of population density.
Table 4.3 lists the expected building densities $\frac{\text{Buildings}}{\text{km}^2} = \frac{\text{pop. dens}}{\text{ppl/unit}} \cdot \varnothing \frac{\text{units}}{\text{building}}$ for the different ACls. Between U1 and U2 and between A2 and A3 remarkably drops of building density occur which are reflected by the above observations.
In reality the ratio of built-up area to empty space is higher in U2 than in U1 (and in A2 higher than in A1) because the building size increases strongly with increasing areal class (a row development building needs much more space than a 1-family house, see [1]).

Possible solution In order to avoid the user's surprise about the more scattered connection points in pixels of higher density a possible solution would be using another connection point symbol (e.g. rectangles) with increasing size for the different building types. This way the plot of load

Table 4.3: Maximum and minimum of expected buildings/km^2 for each areal class

	ACl	R1	R2	U1	U2	A1	A2	A3
max.	$\frac{\text{Buildings}}{\text{km}^2}$	38	41	71	15	16	43	60[a]
min.	$\frac{\text{Buildings}}{\text{km}^2}$	0	28	53	12	13	26	6

[a] A population density of 5000 /km^2 is assumed

connection points would better illustrate the real building situation.
A simple MATLAB implementation could plot the loads depending on their ACl with ACl-specific *'MarkerSize'*-values as *square*-markers *'s'* and the fill color *'MarkerFaceColor'* set to *auto'*. But as (1) a square area would represent some building types inadequately (e.g. row buildings) and (2) the size of the markers remains constant throughout zooming this approach would be only superficial.
It is not the project's aim to model building structures of population areas but to model distribution grids so the visualization of the building density is of very low priority.

Time-consuming drawing of centers of custom size

Observation In order to create ACl areas of custom size and shape the user has to (1) either place multiple centers of the same category close to each other to increase the size of the area or (2) place background-density centers close to the area in order to reshape or scale down the area.
This is (a) very time consuming, (b) fault-prone because the size of a center is not visualized before the placement and (c) the software is unforgiving as steps made are irreversible.

Explanations The distribution grids designed by this software are not required to be real but only realistic at this stage of development. For this reason only the basic design steps with population centers of different densities (and size increasing with density) were implemented and they produce the desired results. A more sophisticated map design was not intended during development.

Possible Solutions Highest priority of the three observations made is (c) the irreversibility. Consequently an *Undo*-Button was added to the *Population center placement*-menubar in parallel to the composition of this section.
To resolve the scaling and shaping problems ((a) and (b)) possible solutions could be implemented:

- The size of the placed center is predefined through user input before placement (only (a), relatively simple)
- Within MATLAB a drawing palette with *draw* and *fill* options is implemented to allow the drawing of individual maps (very and unnecessary complicated)
- The user can load a bitmap file of the population heatmap into MATLAB which is then used for the load placement calculations (complicated (especially to match the colors) but feasible).

A solution to the problem of not displaying the expectable size of the centers before placement is not available as the *Matlab*-function *ginput* does not provide an option to modify the cursor visualization.

Unimportance of relative densities in small maps

Observation For maps with small area the load positions seem to be unaffected by the population centers' and the background's density as shown in Figure 4.3.

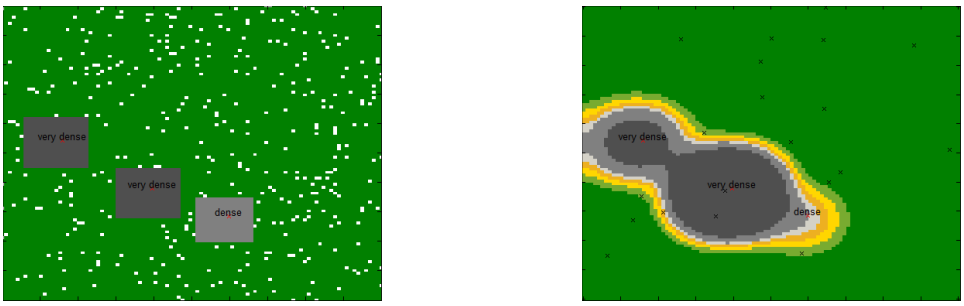

Figure 4.3: Density map before (left) and after (right) smoothing and scaling. Area 1 km^2, inhabitants 200, smoothing factor 50

Explanation This observation is not caused by errors in the algorithm but can be explained by the very small area each pixel represents. The total number of buildings is apportioned to all the pixels so that for each pixel a probability for a building placed on this pixel can be calculated. For the very small pixels' area this probability relatively outweighs the differences in population densities and the loads appear to be distributed totally randomly.

Possible Solution If the user wants to achieve a stronger placement of loads by population density differences he is advised to choose a *zero* background density and to place small population centers at the locations where the loads shall appear.

4.2.4 Commercial/industrial/MV loads

Observation The calculated load map does not include any commercial or industrial loads neither on the LV nor on the MV level.

Explanation As explained earlier no characteristic or average values for these loads were found in literature and the DSO database values for the MV level vary too strongly (as some grids supply airports or steel works) so it can not be used neither.

Possible solutions To include commercial loads into the grid one possibility is to allow the user to set a frequency (e.g. per household) and an average peak demand for commercial buildings.
For industrial loads and MV loads the same approach as for the commercial loads can be adopted or as a second option the user can get the possibility to place particular loads (such as sewage plants, large shopping centers, airports or steel works) and specify the associate peak load similar to the *population center placement* interface.

4.3 LV distribution grid

4.3.1 Results

To evaluate the quality of the generated distribution grid basic load maps were designed for each ACl.
Each load map has 100000 inhabitants and an area derived from the German ACl DS average population density (Appendix A.3, row 7). The background density was chosen in correspondence to the ACl and one population center of the same density was placed in the lower left corner of the map. The user input was set according to Table 4.4.

Table 4.4: User settings for LV grid evaluation

Dialogue	**User input**
Smoothing	0
LV grids	as recommended
LV voltage drop	3%
Interconnections	0
Transformer rating	own sub-grid
Substation placement	geographic center of TSts
Units per Ring	balanced
MV voltage drop	5%
Ring sectioning	TS rating

The resulting characteristic parameters shown in Table 4.5 are normalized by either area or connection points to enable comparison to the DSO database numbers in Appendix A.3.
It has to be noted that the data in Appendix A.3 results from real grids with (1) commercial and industrial loads on both voltage levels and (2) comprises grids of different configuration (radial, open-ring, meshed) and therefore certain discrepancies especially regarding the line length and the transformer rating have to be expected.

Test grid results

Compared to the DSO database the following observations are made:

Inhabitants per CP The averages of inhabitants per connection point deviate strongly from the database numbers. The latter ones are very close to the assumed average of 2.02 inhabitants per household. This is an indication to assume that the connected units listed in the DSO database correspond to households.

CP density The connection point density calculated from the test results differ considerably from the database values:

- The test results for R1 to U1 have around half the density of the database numbers. This might be explained with commercial loads.
- For the ACls U2 to A3 the density is differ strongly from the database values (factor 10 to factor 30). As mentioned in Section 4.2.1 this is most likely explained with the possibly wrong assumption of shared CPs in apartment buildings.

Household density The household density matches the database's CP density very closely (±10%). This observation strongly supports the thesis of non-shared CPs.

CP line distance The average distances between two connection points varies between 100 m to 200 m and exceed the distances provided by Scheffler (Table A.6) by a factors between 4 to 20. The discrepancy between these measured characteristics and those provided by Scheffler has most probably the same explanation as the CP density results.

Line length per connection point The average line length per connection point exhibits the same precision pattern as the inhabitants per connection point:

Table 4.5: Results of the LV grid evaluation

	R1	R2	U1	U2	A1	A2	A3
inhabitants/CP	3.03	4.04	3.41	19.95	20.32	12.15	88.18
CP density [/km^2]	19	31	51	12	13	32	12
hh density [/km^2]	29	61	87	104	134	193	526
CP line distance [m]	159	129	94	211	204	140	206
lines/CP [m]	67	40	23	91	82	35	140
lines/A [km/km^2]	3.1	4.0	4.8	2.6	2.7	4.5	2.4
energy density [MWh/km^2]	86	209	323	201	361	520	870
energy per CP [kWh]	4505	6794	6282	16236	27000	16242	73690
power/CP [MVA]	4	4.15	4.07	23.8	34.05	10.04	90.91
power/hh [MVA]	2.66	2.08	2.41	2.83	3.4	1.67	2.04
avg. S_r [kVA]	100	160	250	400	630	400	630
hh/transformer	37	77	104	139	185	240	308
CP/transformer	25	39	61	17	19	40	7

- For the ACls R1 to U1 the mean line lengths are relatively close to the database values (±10 m).
- For U2 to A3 an increase in line length per connection point is observed in the test results whereas the length decreases for the database data.

The mishandling of the CPs/households connection issue may explain the deviation for the ACls U2 to A3

Line length per area The line length per area measured in the test grids is relatively close to the DSOs' information but surprisingly the resulting length for U2 and A1 are closer to the dataset for R2 and U1 and vice versa. The first of these two cases (relatively few lines calculated for U2 and R1) can partly be explained by the omission of inter-grid connections used more frequently in areas of higher density.
In the database the line length per area of ACl A3 stands out (11.1 km/km^2) from the other ACls. Either the fact that many aged German DS are still configured as meshed operation structure and therefore have more line-km or this number is caused by corrupted data.

Transformer power per CP For the connection point specific transformer power matching numbers can be observed for R1 to U1 but wide differences occur for the remaining ACls.
Possible reasons for the differences of the upper ACl were mentioned already in previous paragraphs.

CPs(/households) per transformer The average number of loads supplied by a TSt was not given in the DSO database. But the average transformer loading can be compared to the calculated maximum values listed in Table 4.1. For all ACls the average number of connected households is only between 40% and 70% of the maximum connectible households.
For the low density ACls this non optimal transformer utilization might be due to the maximum transformer radius. The TSt utilization in high density ACls might be imperfect because of the large demand of the ACl's buildings. See also section Overloading of transformers further below.

Main-feeder length Although Scheffler ([1]) provides information about the average main-feeder length this characteristic is not calculated during grid construction because some main feeders are unproportionally short (see Section 4.3.3).
From the coding perspective a later implementation is simple: Using recursive search the longest possible paths starting from the feeders first node are identified.

Cable cross section

Kerber provides data about typical cross-sections used in German rural and suburban distribution systems and states that each feeder (and sub-feeder) has the same cross-section for all its length. In this project the optimal cross-section (except for the interconnecting lines) is calculated and dimensioned segment-wise (the real approach is not implemented yet). For this reason it is pointless to compare the cross-sections resulting from the grid construction procedure with the literature values in [2, cp. 5.1.2.2.].
On the other hand several test runs of the dimensioning procedure resulted in errors when no cross-section fulfilling the load moment and voltage drop demands existed. This error was caught by dimensioning the respective line section with the largest cross-section available and recording the line dimensioning violation event.
For a maximum voltage drop $\Delta V = 3\%$ the number of violations normalized by the number of TSts ranged between 15 to 20 for the ACls R2, U1 and A2. For R1, U2 and A1 between 8 to 10 violations per TSt were registered and for A3 around 3 violations occurred per TSt. These observations match with the lines per area and the connection points density (Table 4.5) so the one reason for the line violations is the distance between the buildings which strongly affects the load moment. Another reason is that the load moment is calculated based only on the buildings peak load and a flattening of the peak current along the line due to non-coincidence is not taken into account.
Increasing the maximum permissible voltage drop ΔV to 7% reduces the frequency of violations for all classes by 65%.

Overloading of transformers

While testing the module the observation was made that some transformers in A3-networks were overloaded. This phenomenon can be explained by the very large consumers in A3 and is therefore restricted to this ACl:
During the grid construction procedure the number of sub-grids is calculated using the k-means algorithm. Iteratively for every sub-grid the necessary constraints (peak loading and load distance) are checked until met.
After every check k is increased by 1 under the approximate assumption that adding another cluster never increases but only reduces the peak loading and load distance in each cluster. This assumption does not hold properly for A3 as it can happen that one of the analyzed sub-grid's large consumers is assigned to an already checked sub-grid while performing the next clustering. As the sub-grid conditions are not checked a second time after the iteration the overloading of transformers can occur.
Up to now the overloading violations are only registered. In later module updates a computing-efficient constraint verification for all sub-grids after each clustering step can be taken into consideration.

4.3.2 LV grid computation time

During the construction of the test grids the computation time listed in Table 4.6 was measured. The computation time decreases with the decreasing number of connection points and as it can be seen in Table 4.6 the calculation time per CP or per TSt only varies in the range of ms.
This observation can be explained by the complexity of the k-means algorithm $\mathcal{O}(n^{k+1} \cdot \log n)$ and the complexity of the MST algorithm $\mathcal{O}(l+n \cdot \log n)$ (number of loads n, number of lines l).

Table 4.6: Computation time for the construction of the LV test grids

	R1	R2	U1	U2	A1	A2	A3
avg. calculation time [s]	70	25	20	25	17	9	12
calculation time/CP [ms]	2.15	1.05	0.63	4.15	3.47	1.03	10.76
calculation time/TSt [ms]	53	41	39	69	64	41	74

4.3.3 Scope for improvement

Edgy cable routing

Observation During software testing the edgy cable routing attracted attention. In practice cables routes are mainly laid below roads and follow their course but different to the real situation where most crossroads and side roads branch off perpendicularly the implemented MST assumes the shorter direct route and thereby creates an edgy cable network which hardly can be associated with a street-map.

Explanation The MST algorithm always picks the nodes to connect by the shortest available distance. The input distances are the calculated euclidean distances between the nodes and therefore the direct linear distance between two nodes is used for solving the MST and calculation of the line length.

Possible solution One possible solution to this problem (especially for more modern city with only rectangular road branches) is the usage of the (partly implemented) *cityblock* metric instead of the *euclidean* metric. In this case all distances are calculated as *cityblock* distances, the MST algorithm determines the minimum spanning tree based on these distances and instead of k-means the k-median algorithm is used for clustering. It is very likely that this increases the observed line length considerably.
The implementation of the visualization (plotting) of the lines may turn out to be very challenging as two possible routes exist for each line. Furthermore the lines' edges should then be added to the node list in order to avoid

double lines and to minimize the total line length.
A very sophistic implementation would even allow branch-offs from every segment of existing lines (as implemented in the LabView Block Diagram GUI). This approach on the other hand would not be solvable with the MST any more as the number of nodes becomes very large.

Very short main feeders

Observation Throughout software testing it was observed that some of the main feeders emanating from the TSts were very short and only supplied between 1 to 3 loads. This does not reflect a real grid where this short feeder would branch off from a main feeder.

Explanation This behavior is due to the programming of the MST algorithm. The number of leaving feeders O_T and the equivalent starting nodes (loads) are pre-calculated before the MST is executed on the group of the starting nodes. In this procedure it can easily happen that one of the feeders gets sealed in by the adjacent feeders and ends dead quickly.

Possible solutions One possible solution is to allocate the TSt' loads to O_T sectors and to calculate the MST for each sector (the loads closest to the TSt are starting nodes). This approach may balance the feeder length better but on the downside it sabotages line length minimization and therefore this approach was not implemented. A possible sectoring approach is described in [32], see also Section 4.4.3)
Another solution is to find the O_T nodes closest to the transformer and to build up O_T trees by adding each round one nearest node to each of the trees. In a final step the trees are connected to the transformer. This approach guarantees feeders of the approximately same length.
Difficulties arise when one node is the nearest node for more than one tree. In this case it is necessary to compare all possible solutions of connecting one node (from the common pool of unconnected nodes) to O_T pools of connected nodes) and to identify the combination minimizing the sum of the O_T new connections.
As this idea came up in the final phase of the work it was not possible to implement it properly any more. Furthermore the calculation effort of comparing all possible solutions in each step might exceed the implementation of a previous sectoring while not providing better results.

4.4 MV distribution grid

4.4.1 Results

The lack of reference literature comprising characteristic data on MV distribution grids prevents a quantitative comparative analysis of the resulting MV grids.

Test grid results

The results of the analysis of the test grids (Section 4.3.1) are shown in Table 4.7.

Table 4.7: Results of the MV grid evaluation

	R1	R2	U1	U2	A1	A2	A3
TSt density [/km^2]	0.77	0.8	0.84	0.75	0.72	0.8	1.65
TSts/ring	63	58	60	59	53	52	55
rings/area [/1000 km^2]	12	14	14	13	14	16	31
lines/A [km/km^2]	1.29	1.22	1.16	1.13	1.10	1.12	1.66
TSt line distance [km]	1.64	1.51	1.36	1.49	1.49	1.38	0.95

It can be observed that for this high population enough TSts exist so that for all ACl the rings connect up to the maximum permissible number of TSt (64) even though the option *balanced rings* was chosen.
The accumulation of rings per area reflects the same pattern as the TSt density: For all but A3 the TSt density is around 0.8 /km^2 but in A3 the density doubles due to the much higher energy density in A3 (Table 4.5).
The average line distance between TSts reflects a similar pattern as the last two characteristics: For R1 to A3 the average length ranges between 1.35 km to 1.65 km but only is about 1 km in A3.
The average households share at the coincident peak power in a 100000 persons grid is calculated to 1.2 kW which is close to the maximum 15-minute peak average of a 4000 kWh SLP household (Appendix B.2)

Line dimensioning

Tests showed that the maximum available cross-section of 400 mm^2 is too small for the MV rings when up to 64 TSts can be connected to one single ring and when only one SSt has to supply all TSts (long distances).
Another dimensioning approach would consider only the TSts' share of the maximum coincident demand which would probably result in smaller cross sections. But as long as the short-circuit current capacity is not verified during cable sizing (Section 2.2.3) this more conservative approach should be utilized.

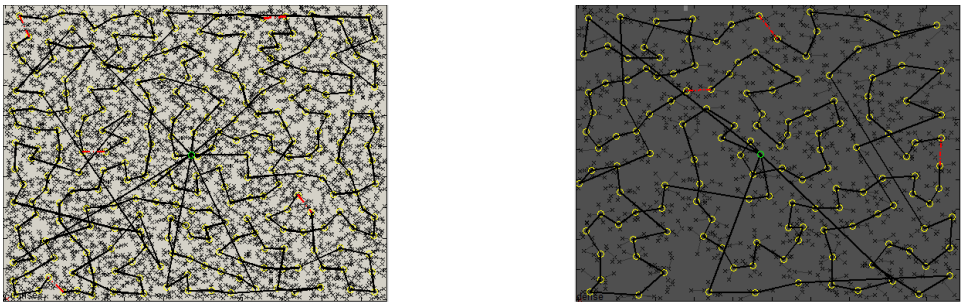

Figure 4.4: Exemplary grids illustrating the MV routing

4.4.2 MV grid computation time

The time needed for the modeling and sizing of the MV was negligible short (<0.1 s) in all test cases. This is mainly thanks to the very fast VRP routing algorithm.

4.4.3 Scope for improvement

Line routing

Observation Throughout most of the created test distribution grids the quality of MV line routing was unsatisfactory.
As illustrated in Figure 4.4 rings (1) have one far above-average long feeder section leaving the SSt (2) intersect with lines of other rings and (3) form circle by crossing over their own lines (non planar).
All three observations lead to projecting unnecessary many km of MV lines.

Explanation All three findings are caused by the greedy Nearest-Neighbor VRP implementation.
The overly lengthy line section connecting to the SSt (1) is created as soon as the algorithm realizes that the intended number of TSts is lined up on the ring and it has to return to the SSt.
Intra- (2) and inter-ring (3) intersections occur because the algorithm does (2) not optimize towards minimizing the rings total length but only the distance to each next element and (3) because the rings are not filled up with TSts in parallel but subsequently (so the later a ring is constructed the longer it becomes).
For TSP problems the Nearest-Neighbor solutions are in average 25% longer than the optimal solution for VRP this number is estimated to be larger [33].

Possible solutions The non-optimal MV grid structure is only caused by the simple but very fast VRP algorithm used so the algorithm depth has to be improved in order to improve the grid.
To avoid the abrupt return to the SSt (1) algorithms improving the routing

iteratively (e.g. based on *Lin-Kernighan heuristics)*, *ant colony optimization*, *simulated annealing* or genetic algorithms shall better be used. In [34] the latter two solutions are explained and analyzed, [29] describes a three step approach to expansion planning of underground power grids which can be transferred to initial planning too. These solution algorithms listed above should also solve the rings' self-crossing (2).
In order to avoid intersections of different rings (3) a preallocation of the TSts to rings can be useful. Whilst k-means is not applicable in this case as some clusters might be in large distance of the SSt the segmentation method discussed in [32] is a reasonable approach.
Given this segmentation comprises that each segment does not comprise more than the maximum TSts per ring each segments ring can be used with a TSP algorithm instead of using the VRP solutions.

Multiple Substations

Observation As described earlier this software module assumes that one single substation supplies the whole distribution system.

Possible solution In [35] three different MATLAB implementations of Multi-Depot vehicle routing problem algorithms based on meta-heuristics are presented.
After determining the necessary number of substation, e.g. by setting a maximum substation rating, such an algorithm would allow the construction of a line length minimization network with multiple SSt.
To allow rings connecting two different substations the implementations described in [35] would only have to upgraded so that "the vehicles are allowed to return to any depot instead of only to the start depot".

MV ring capacity

Observation In the current MV grid calculation the TSt capacity of ring is determined by a fixed number. It may probably be more reasonable to determine the maximum number of TSt individually for each ring based on a maximum ring loading.

Possible Solution Given a maximum ring capacity $S_{rg,\text{limit}}$ the maximum "vehicle capacity" in the implemented VRP algorithm has to be changed from the current limit of 64 TSt to $S_{rg,\text{limit}}$. This is a basic functionality of VRP algorithms and the only reason it is not yet implemented is the absence of values for the maximum capacity.

Chapter 5

Conclusion and future work

As described in Section 1.2 the aim of this project is developing a software module which is able to generate realistic distribution grid topologies.
To differentiate between different types of distribution systems a classification based on the population density was introduced. Although it was not possible to show statistical significance of this classification the resulting test DSs widely confirm this classification.
The provided GUI allows the user to easily design spatial density maps which deduces the spatial load distribution.
Subsequently the software calculates the number of necessary transformer and, depending on the users preferences, constructs the low voltage grid in radial or partly open-ring configuration before dimensioning lines and transformers in order to allow secure operation. Test runs show that most of the calculated grid structures resemble real distribution systems, only the results from test runs of the most dense areal class differ considerably from the real grids.
On the medium voltage level a simple algorithm connects the transformer stations in rings to one single substation. The dimensioning of the MV lines is not fully developed but solutions are proposed.
The total construction of a large DS can be done within a few minutes as the design of the spatial map, the computation of the LV lines and the dimensioning of the lines are the only time intensive steps during the procedure.
All in all the developed module constructs solid DSs with minor shortcomings.
Future work should eliminate these shortcomings described in Section 4.2.3 and Section 4.3.3 and then focus on improving and upgrading the modules functionality. Especially the MV grid construction algorithm should be enhanced as proposed in Section 4.4.3. Subsequent work is recommended to approach the problem of missing industrial, commercial and MV loads by identifying there expected size and frequency for the different ACl and including them into the routine.

Appendix A

Settlement classification

A.1 BSSR classification (Germany)

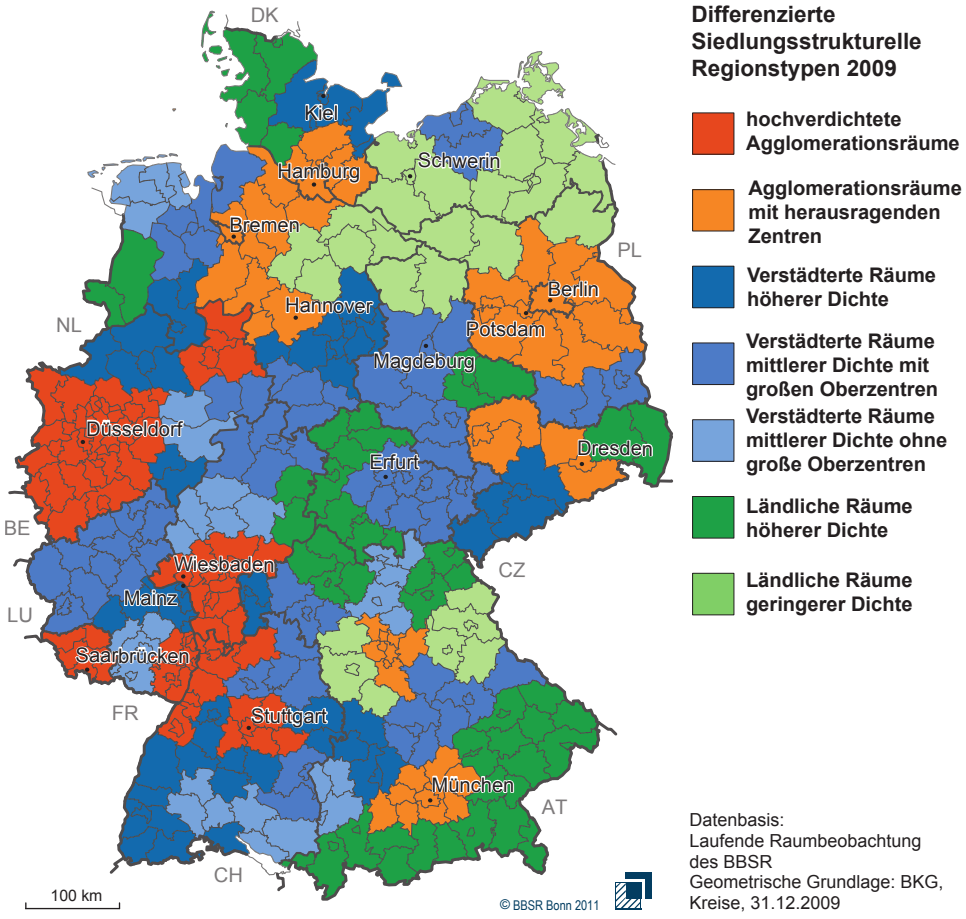

Figure A.1: Differentiated settlement classification of regions 2009

A.2 Grid characteristics [1] and [2]

The following tables show data from Scheffler's dissertation fitted into this projects classification according to Table 2.2 [1].

A.2.1 Transformer characteristics

Table A.1: Typical transformer station ratings

S_r [kVA]	R1	R2	U1	U2	A1	A2	A3
630		630	**630**	**630**	**630**	**630**	**630**
400		**400**	**400**	400		400	
250	250	**250**	250				
160	**160**	160					
100	100						
50	50						

Table A.2: Feeder outlets of TSts, mean and standard deviation

feeders	R1	R2	U1	U2	A1	A2	A3
μ	2.2	2.8	4.6	4.4	4.3	5.0	5.8
$\pm\sigma$	0.7	0.8	1.9	1.5	1.6	2.1	0.8

A.2.2 Load characteristics

Table A.3: Yearly electricity consumption per household, mean and standard deviation (no confidence interval).

energy	R1	R2	U1	U2	A1	A2	A3
μ [kWh]	3026	3423	3834	1853	2716	2716	1698
$\pm\sigma$ [kWh]	1078	1368	516	977	489	916	411

Table A.4: Housing units per connected building [1]

$\frac{\text{units}}{\text{building}}$	R1	R2	U1	U2	A1	A2	A3
μ	1.3	1.8	1.4	8.5	9.2	5.7	41
range	1–2	1–6	1–6	6–60	6–15	2–12	20–80

A.2.3 Line characteristics

Table A.5: Usage of conductor cross-section according to [2]

mm^2	R	U	A
185			20%
150	36%	84%	54%
120			15%
95	18%	4%	
70	21%	6%	
50	19%		
other	7%	5%	12%

Table A.6: Distances between buildings' service connections, mean and standard deviation

distance	R1	R2	U1	U2	A1	A2
μ [m]	48	37	16	24	31	13
$\pm\sigma$ [m]	29	17	7	8	12	7

The distances between the buildings' service connections correspond to the width's of of the buildings' lands facing public place.

A.3 Grid structure German DSO database

The DSOs database is supposed to contain the following grid characteristics for each voltage level and DSO: geographic and supplied area, total length cables, total length OHLs, installed transformer power, peak load, yearly energy, grid losses, number of connected loads and inhabitants. The following problems arose from the database analysis:

- Supplied area (from land-use statistics) is not specified for most DSOs
- The database implied a code indicating the inclusion of service laterals but as the decoding was not explained the code is ignored
- the list of installed transformer power is incomplete (798 MV/LV-transformer sets but 853 LV grid sets)
- Loss information data is of insufficient quality

The following table displays the grid characteristics analyzed for the areal classes specified in Table 2.2

	∅ LV	R1	R2	U1	U2	A1	A2	A3	∅ MV
samples	853	61	72	71	61	52	150	335	803
geogr. area A [km^2]	506	2137	1711	863	203	481	152	81	500
connected loads CPs	62526	98876	124216	87890	23420	73023	30603	622592	6910
*CP density [/km^2]	333	42	68	95	122	147	216	613	2
inhabitants	100968	149710	212363	132958	43883	127669	56754	99709	101824
*pop. density [/km^2]	570	58	124	175	210	272	389	1038	622
*inhabitants/CP	1.95	1.76	1.99	1.99	1.98	2.07	2.01	1.95	894
cables [km]	1250	2539	3911	1866	685	1335	639	817	497
OHLs [km]	158	565	396	292	51	406	85	40	141
*lines/CP [m]	31	63	36	33	34	30	28	23	3585
*lines/A [km/km^2]	6.9	2.5	2.2	2.9	3.8	3.9	5.6	11.1	2.6
(peak load P_{pk} [MW])[a]	*(592)*	*(14)*	*(62)*	*(5349)*	*(21)*		*(125)*	*(17)*	*(17)*
**(P_{pk}/CP [kW])*	*(7.41)*	*(10.9)*	*(1.6)*	*(2.0)*	*(2.5)*		*(1.4)*	*(1.2)*	
yearly energy E [GWh]	271	381	573	386	116	430	133	251	897.8
*energy density [MWh/km^2]	1802	520	313	328	589	831	952	3433	14480
*energy per CP [kWh]	6321	11974	4925	4898	5148	5599	4792	6676	$15.9 \cdot 10^6$
power installed [GVA]	245	470	613	342	99	295	121	208	
*power/CP [MVA]		4.75	4.93	3.89	4.25	4.03	3.95	3.32	

[a]based on very few data. Do not use results! *derived characteristics

Appendix B

Load modeling

Table B.1: BDEW standard load profiles SLPs

SLP	description
G0	general commerce (weighted average of G1-G6)
G1	commerce workdays 8 a.m. to 6 p.m.
G2	commerce with severe-to-predominant consumption in the evenings
G3	commerce with 24-hours consumption
G4	shops, hairdressers
G5	bakeries with baking room
G6	weekend commerce
L0	general farm (weighted average of L1-L2)
L1	farms with dairy sector
L2	other farms
H0	general household

Table B.2: Households' maximum power consumptions in literature

Source	peak	context
[36]	1.92 kW	average power of maximum 15-minute energy consumption of a 4000 kWh household
[13]	4.5 kW	50 W/m^2 and an average household size of 90 m^2
[2]	30 kW	based on [37] (often cited in this context)
[17]	18 kW	Student project. For n households per building multiply with $f = n^{-0.52}$ to account for load coincidence
[4]	13 kW	reference benchmark grid consumer
[1]	2 kW	evening peak in daily power consumption diagram (exemplary household)

Appendix C

Line dimensioning

Cross-section–load moment diagram and table for ΔVs [23]:

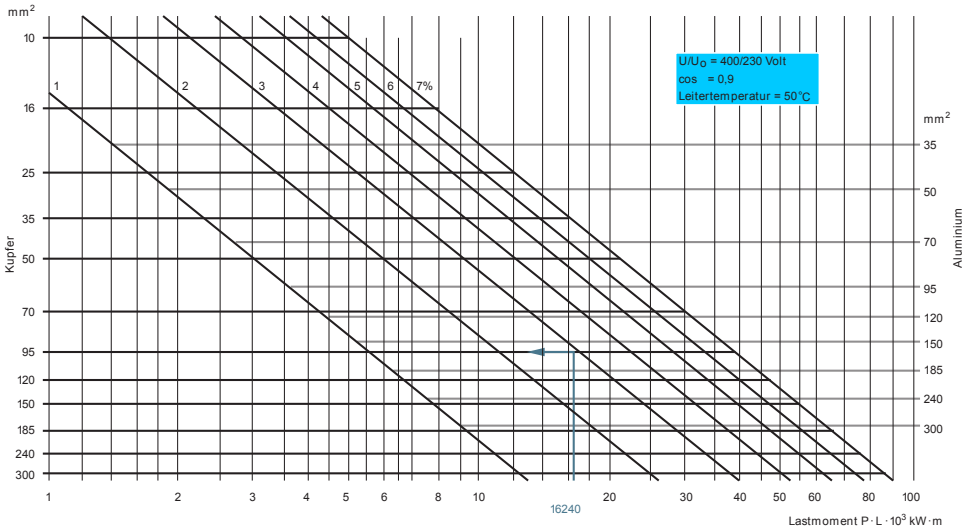

Table C.1: Max. load moment by ΔV and aluminum cross-section

	max load moment [kW m] by voltage drop ΔU						
cross-section	7%	6%	5%	4%	3%	2%	1%
35 mm^2	10028	8475	7206	5704	4324	2821	1416
50 mm^2	13420	11393	9643	7645	5796	3792	1909
70 mm^2	18947	16085	13655	10842	8224	5362	2724
95 mm^2	25394	21655	18302	14552	11066	7207	3623
120 mm^2	30946	26350	22303	17787	13505	8757	4435
150 mm^2	36552	30985	26227	20916	15904	10359	5200
185 mm^2	43951	37591	31724	25337	19266	12586	6290
240 mm^2	52927	45066	38089	30512	23098	15112	7563
300 mm^2	63076	54029	45029	36417	27691	18090	9026

Appendix D

Software module

D.1 Parameters

Table D.1: Constant values loaded via *fixed_parameters.m*

name	table	description
R1... A3	2.2	population classes and densities
E_h	2.3	yearly class specific household consumption [kWh]
hh_cp	2.3	household variation by class
t_o	A.2	average number of transformer outlets by class
l_cross	C.1	cross-section specific load moment limits [kW m]
Cmap	2.2	discrete colormap based on classification

Table D.2: Default values of parameters loaded via *user_parameters.m*

name	default	description
res	100	resolution of both x and y coordinates
P_pk	18	Average peak load of a single household [kW]
PpHH	2.02	Average people per household
g_coinc	0.06	coincidence factor
lam	0.9	power factor
CP_Max	500	Maximum number of connection points per TSt
distance	*eucl.*	calculation method for the distance matrix
d_max	0.7	maximum direct distance of CP from the TSt [km]
l_SgSg	2	maximum interconnections to other sub-grids
T_rg_max	64	maximum number of TSt connected to one MV ring
dU_LV	3	maximum voltage loss along LV lines
dU_MV	3	maximum voltage loss along MV lines

D.2 GUI handling of data

Table D.3: Descriptions of the GUIDE *handles.*-elements used in the module

elements containing figure-handles	
Main_Gui	Main GUI
Map_axes	plot area
datatable	table below the plot area
menu_show	(*Menu bar*→)*Show*-Menu
menu_project	(*Menu bar*→)*Project*-Menu
uitoolbar1	Toolbar module
grid_MV	(*Menu bar*→*Show*→) *MV Grid*-Option
grid_LV	(*Menu bar*→*Show*→) *LV Grid*-Option
CP_MV	(*Menu bar*→*Show*→) *MV Loads*-Option
CP_LV	(*Menu bar*→*Show*→) *LV Loads*-Option
show_heatmap	(*Menu bar*→*Show*→) *Heatmap*-Option
show_centers	(*Menu bar*→*Show*→) *Pop Centers*-Option
Open	(*Menu bar*→*Project*→)*Open Project* (only callback used)
Save	(*Menu bar*→*Project*→) *Save Project*
New	(*Menu bar*→*Project*→) *New Project*
toolbar_showgrid	(*Toolbar*→)*Show Grid*-Button
legend	(*Toolbar*→)*Show Legend*-Button
colorbar	(*Toolbar*→)*Insert Colorbar*-Button
datacursor	(*Toolbar*→)*Data Cursor*-Button
zoomin	(*Toolbar*→)*Zoom in*-Button
zoomout	(*Toolbar*→)*Zoom out*-Button
pan	(*Toolbar*→)*Pan*-Button
SaveTbar	(*Toolbar*→)*Save Project*-Button
elements containing data	
output	Default: Address of the main GUI
LV_L	Cell array: LV lines matrices (output 2)
LV_CP	Cell array: LV CPs matrices (output 1)
MV_L	Cell array: MV lines matrices (output 4)
MV_CP	Cell array: MV CPs matrices (output 3)
centers	Matrix: type and position of population centers
LV_LD	Cell array: LV loads (for plotting)
LV_Lc	Cell array: closed LV lines (for plotting)
LV_Lo	Cell array: open LV lines (for plotting)
MV_LD	Cell array: MV loads(TSts) (for plotting)
MV_Lc	Cell array: closed MV lines (for plotting)
MV_Lo	Cell array: open LV lines (for plotting)
legend_data	Matrix: data from the table (output 5)

D.3 Grid building procedure

Exemplary construction of a distribution grid in the size of the German *Landkreis* with an area of approximately 1000 km^2 and 127000 Inhabitants living in 25 municipalities.

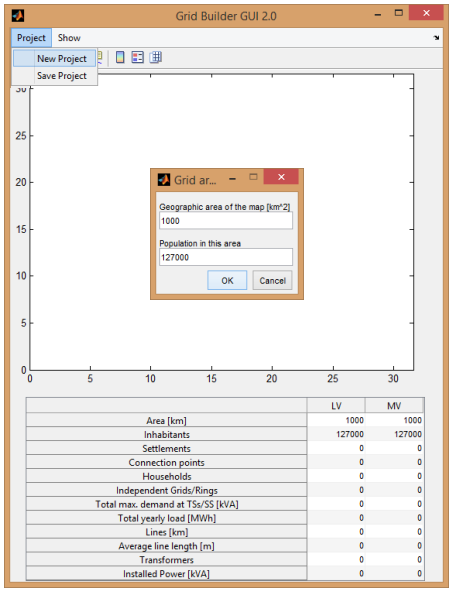

Figure D.1: **Initialization of a new project.** Input of size and inhabitants of the supplied area.

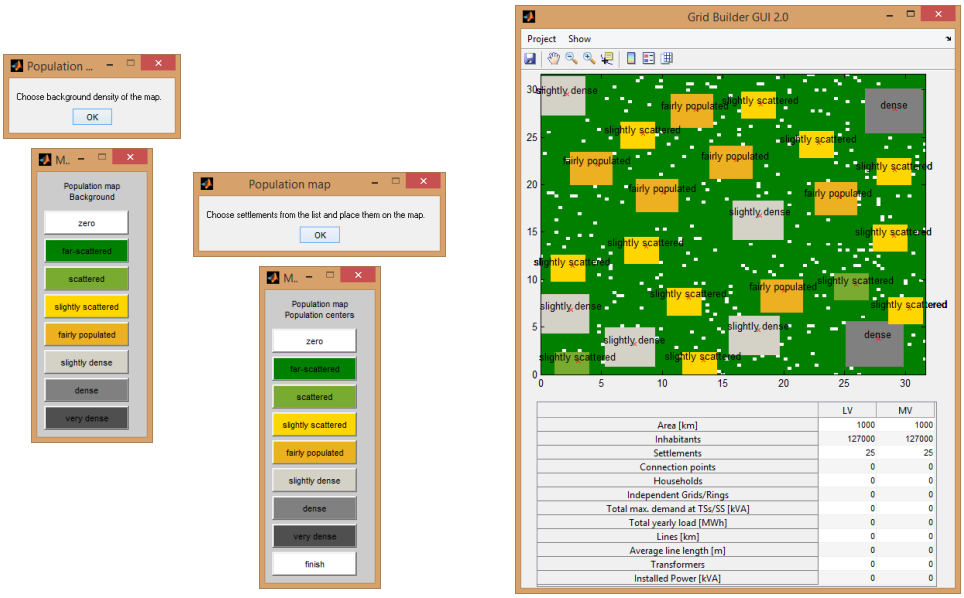

Figure D.2: **Design of the spatial map.** Definition of the relative background density and population centers.

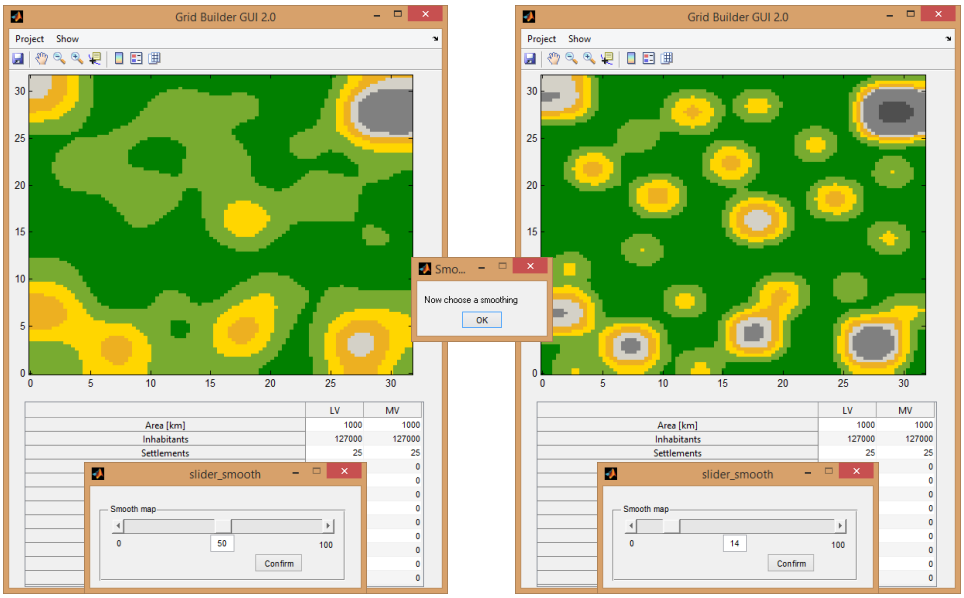

Figure D.3: **Smoothing the spatial map.** In order to flatten out the population density gradient.

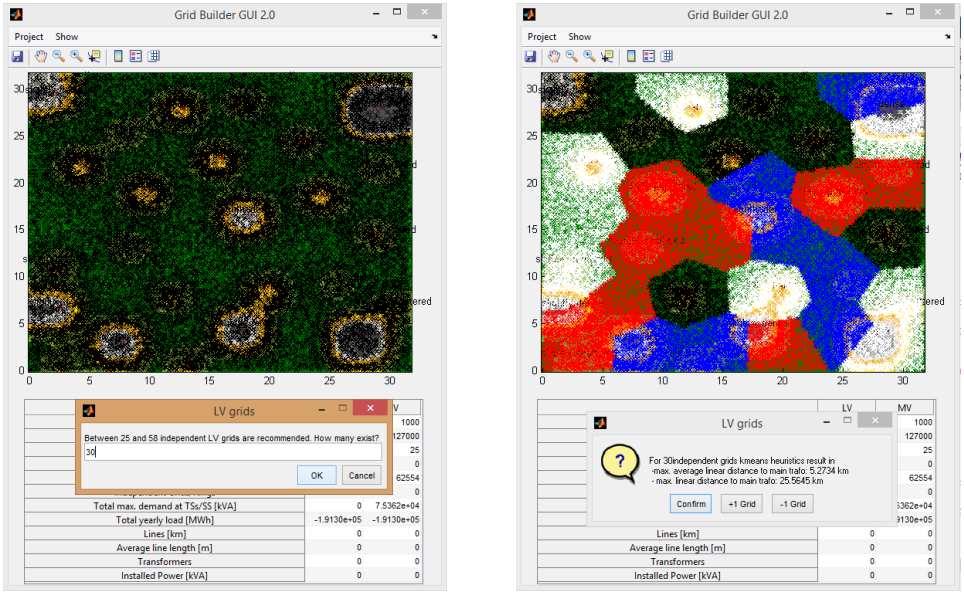

Figure D.4: **Amount of independent LV grids.** After calculation of the LV loads the number of independent grids is user-set.

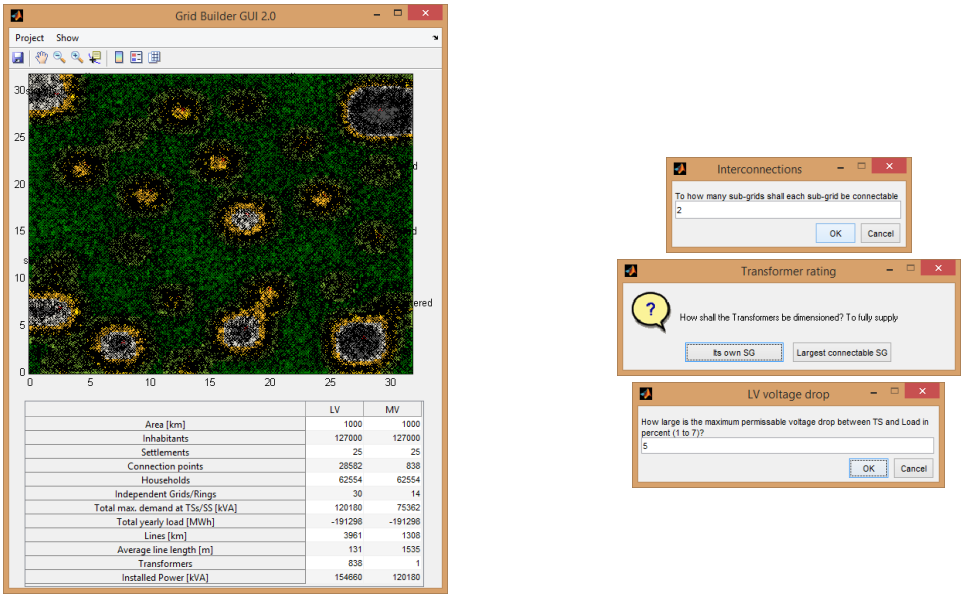

Figure D.5: **LV grid design options.** For the dimensioning of transformers and lines the user sets three different options.

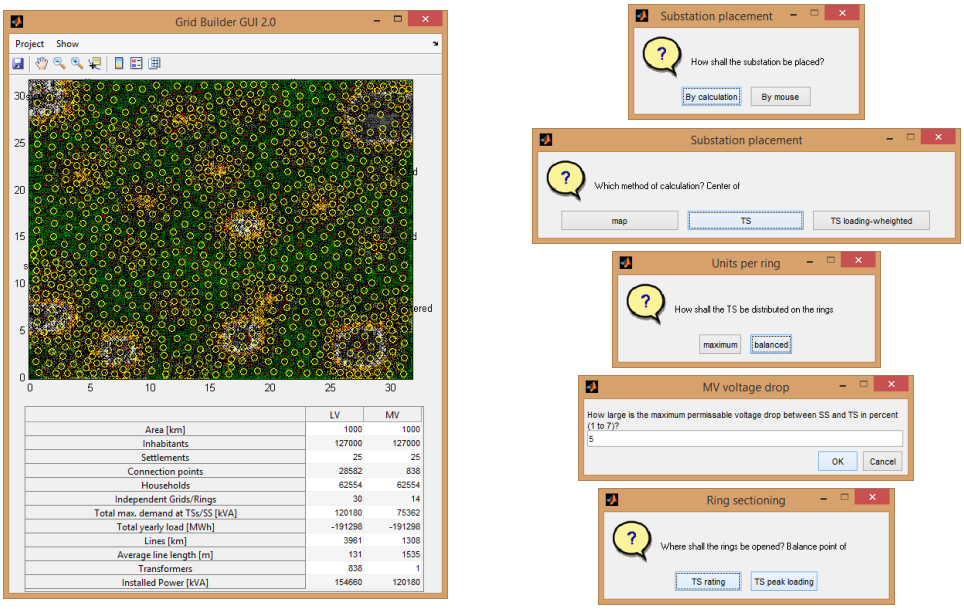

Figure D.6: **MV grid design options.** For the layout of the MV grid and dimensioning of the substation and the lines the user sets up to five different options.

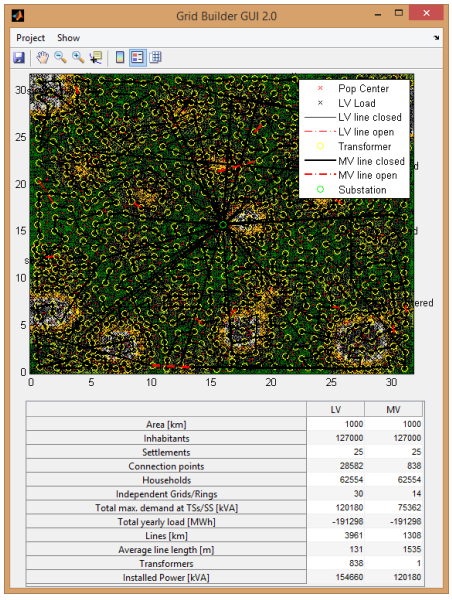

	LV	MV
Area [km]	1000	1000
Inhabitants	127000	127000
Settlements	25	25
Connection points	28582	838
Households	62554	62554
Independent Grids/Rings	30	14
Total max. demand at TSs/SS [kVA]	120180	75362
Total yearly load [MWh]	-191298	-191298
Lines [km]	3961	1308
Average line length [m]	131	1535
Transformers	838	1
Installed Power [kVA]	154660	120180

Figure D.7: Illustration of the complete distribution grid.

Bibliography

[1] J. Scheffler, *Bestimmung der maximal zulässigen Netzanschlussleistung photovoltaischer Energiewandlungsanlagen in Wohnsiedlungsgebieten.* PhD thesis, Technische Universität Dresden, 2002.

[2] G. Kerber, *Aufnahmefähigkeit von Niederspannungsverteilnetzen für die Einspeisung aus Photovoltaikkleinanlagen.* PhD thesis, Technische Universität München, 2011.

[3] S. Koch, A. Ulbig, and F. Ferrucci, "An innovative software platform for simulation and optimization of active distribution grids for DSOS and smartgrid researchers," in *CIRED Workshop 2014*, 2014.

[4] S. Papathanassiou, N. Hatziargyriou, and K. Strunz, "A benchmark low voltage micgrogrid network," in *CIGRE Symposium - Power systems with dispersed generation: technologies, impacts on development, operation and performances*, 2005.

[5] W. Kersting, "A comprehensive distribution test feeder," in *Transmission and Distribution Conference and Exposition, 2010 IEEE PES*, pp. 1–4, April 2010.

[6] K. Rudion, A. Orths, Z. A. Styczynski, and K. Strunz, "Design of Benchmark of Medium Voltage Distribution Network for Investigation of DG Integration," in *Power Engineering Society General Meeting*, IEEE, 2006.

[7] H. Rui, A. M., and W. Wellssow, "Synthetic Medium Voltage Grids for the Assessment of Smart Grid Techniques," in *3rd IEEE PES Innovative Smart Grid Technologies Europe (ISGT Europe), Berlin*, 2012.

[8] P. Schulz, J. Heitzig, and K. Jürgen, "A random growth model for power grids and other spatially embedded infrastructure networks," *Eur. Phys. J. Special Topics*, vol. 223, pp. 2593–2610, 2014.

[9] "Verordnung über den Zugang zu Elektrizitätsversorgungsnetzen (StromNZV) §17."

[10] "Verordnung über die Entgelte für den Zugang zu Elektrizitätsversorgungsnetzen (StromNEV) §27."

[11] A. A. Sallam and O. P. Malik, *Electric Distribution System*. IEEE Press Series on Power Engineering, Wiley, 2011.

[12] J. Schlabbach and K.-H. Rofalski, *Power System Engineering, Planning Desing and Operation of Power Systems and Equipment*. Wiley-VCH, 2014.

[13] G. Lipphardt, *Elektrische Anlagen und Netze*. Hochschule Mannheim, 2006.

[14] H. Janich, "Laufende Raumbeobachtung - Raumabgrenzungen, Siedlungsstrukturelle Regionstypen." Online, 2011.

[15] A. J. Schwab, *Elektroenergiesysteme : Erzeugung, Transport, Übertragung und Verteilung elektrischer Energie*. Springer Berlin, 2. ed., 2012.

[16] W. H. Kersting, *Distribution System Modeling and Analysis*. Electric Power Engineering, CRC Press, 2002.

[17] P. Forjan, G. Schriebl, and W. C. Schuster, "Energieverteilung in Hoch-, Mittel- und Niederspannungsnetzen," Master's thesis, HTBL u. VA BULME Graz-Gösting, 2006.

[18] "Three-phase oil-immersed distribution transformers 50 hz, from 50 kva to 2500 kva with highest voltage for equipment not exceeding 36 kv - part 1: General requirements; german version en 50464-1:2007."

[19] "Iec 60076-7:2005 power transformers - part 7: Loading guide for oil-immersed power transformers."

[20] H. Kiank and W. Fruth, *Planning Guide for Power Distribution Plants: Design, Implementation and Operation of Industrial Networks*. Publicis Publishing, 2011.

[21] U. Post, "Grundlagen der Energietechnik: Netze und Betriebsmittel - Netzformen." Online, Coursescript, September 2007.

[22] T. Haase and H. Weber, "Optimierung von Mittelspannungsnetzen regionaler Energieversorger," in *10.Symposium Maritime Elektronik*, pp. 147–150, Arbeitskreis Energie- und Steuerungstechnik, 2001.

[23] Infrastruktur Kabelsysteme, "Auslegung Kabelsysteme," tech. rep., Brugg Cables, 2014.

[24] "En 50160:2011-02, voltage characteristics of electricity supplied by public distribution networks; german version en 50160:2010."

[25] J. Nešetřil and H. Nešetřilová, "The Origins of Minimal Spanning Tree Algorithms – Borůvka and Jarník," *Documenta Mathematica*, vol. Extra Volume ISMP, pp. 127–141, 2012.

[26] Y. Backlund and J. Bubenko, "Distribution System Design Using Computer Graphics Technique," in *Power Industry Computer Applications Conference, 1979. PICA-79. IEEE Conference Proceedings*, pp. 382–388, May 1979.

[27] R. Prim, "Shortest Connection Networks And Some Generalizations," *The Bell System Technical Journal*, vol. 36, pp. 1389–1401, 1957.

[28] A. K. Jain, M. N. Murty, and P. J. Flynn, "Data clustering: A review," *ACM Comput. Surv.*, vol. 31, pp. 264–323, Sept. 1999.

[29] Z. Bozic and E. Hobson, "Urban underground network expansion planning," *Generation, Transmission and Distribution, IEE Proceedings-*, vol. 144, pp. 118–124, Mar 1997.

[30] G. Reeves, "smooth2a.m." Matlab File Exchange, March 2009.

[31] P. Wied, "heatmap.js." Online, October 2014.

[32] T. Okraszewski, G. Balzer, and C. Schorn, "Restructuring of the existing medium voltage cable networks using segmentation method - Impact on networks reliability," in *CIRED, 19th International Conference on Electricity Distribution*, 2007.

[33] D. S. Johnson and L. A. McGeoch, "The traveling salesman problem: A case study in local optimization," *Local search in combinatorial optimization*, vol. 1, pp. 215–310, 1997.

[34] A. Kovács, "Solving the Vehicle Routing Problem with Genetic Algorithm and Simulated Annealing," Master's thesis, Högskolan Dalarna, Sweden, May 2008.

[35] T. C. M. Caldeira, "Optimization of the Multi-Depot Vehicle Routing Problem: an Application to Logistics and Transport of Biomass for Electricity Production," Master's thesis, Universidade Técnica da Lisboa, October 2009.

[36] BDEW, "Lastprofilverfahren Strom." Excel-Sheet, December 2014.

[37] W. Kaufmann, *Planung öffentlicher Elektrizitätsverteilungssysteme*. VDE, 1995.